MARIA IZABEL COSTA DE NOVAES

Physiological and Biochemical Aspects of Soybean Sprayed with Manganese Phosphite for the White Mold Control

Dissertação apresentada à Universidade Federal de Viçosa, como parte das exigências do Programa de Pós-Graduação em Fitopatologia, para obtenção do título de *Magister Scientiae.*

VIÇOSA

MINAS GERAIS – BRASIL

2016

Ficha catalográfica preparada pela Biblioteca Central da Universidade Federal de Viçosa - Câmpus Viçosa

T
N935p
2016

Novaes, Maria Izabel Costa de, 1991-
Physiological and Biochemical Aspects of Soybean Sprayed with Manganese Phosphite for the White Mold Control / Maria Izabel Costa de Novaes. – Viçosa, MG, 2016.
ix, 50f. : il. (algumas color.) ; 29 cm.

Orientador: Fabrício de Ávila Rodrigues.
Dissertação (mestrado) - Universidade Federal de Viçosa.
Inclui bibliografia.

1. Soja - Doenças e pragas - Fungo. 2. Soja - Doenças e pragas - Controle bioquímico. 3. Soja - Doenças e pragas - Controle biológico. 4. *Sclerotinia sclerotiorum*. 5. Soja - Efeito do manganês. 6. Soja - pulverização. 7. Troca gasosa em plantas. I. Universidade Federal de Viçosa. Departamento de Fitopatologia. Programa de Pós-graduação em Fitopatologia. II. Título.

CDD 22 ed. 633.3494

MARIA IZABEL COSTA DE NOVAES

Physiological and Biochemical Aspects of Soybean Sprayed with Manganese Phosphite for the White Mold Control

Dissertação apresentada à Universidade Federal de Viçosa, como parte das exigências do Programa de Pós-Graduação em Fitopatologia, para obtenção do título de *Magister Scientiae.*

APROVADA: 21 de julho de 2016.

Hélvio Gledson Maciel Ferraz

Lucas Magalhães de Abreu

Renata Sousa Resende
(Coorientadora)

Fabrício de Ávila Rodrigues
(Orientador)

À Deus,

pela benção da vida e por iluminar meus caminhos em todos os momentos.

Aos meus pais,

pelo amor incondicional, carinho e confiança depositados para que mais um desafio fosse vencido,

Dedico

Jesus, Tu és o Santíssimo Sacramento de minha alma, mesmo nos dias de provação, de sofrimento e de lágrimas. Perto de Tí Jesus, tudo é bom!

Pe. Roberto Lettiere

AGRADECIMENTOS

À Deus por minha vida, família e amigos.

À Universidade Federal de Viçosa, ao Departamento de Fitopatologia e ao Programa de Pós-Graduação em Fitopatologia por disponibilizarem os recursos necessários para a realização deste trabalho.

A Comissão do Conselho Nacional de Desenvolvimento Cientifico e Tecnológico - CNPq, pelo apoio financeiro.

Aos meus pais, Aurindo e Cassia, maiores incentivadores e apoiadores dos meus estudos e sonhos. Ao meu irmão João Vitor e toda minha família, pelo amor, incentivo e apoio incondicional.

Ao meu namorado Renato por andar de mãos dadas comigo, confiando, incentivando e participando de cada conquista.

Ao Professor Fabrício de Ávila Rodrigues pela confiança, incentivo, paciência e pelos incontáveis momentos de compreensão e ensinamentos.

Ao Dr. Daniel Debona pela ajuda, dedicação, amizade e contribuições para condução deste trabalho.

Aos meus amigos do Laboratório da Interação Planta-Patógeno pelo companheirismo, troca de experiências e ajuda durante os experimentos.

Aos Professores do Departamento de Fitopatologia pelos ensinamentos, amizade e pela sabedoria que não encontramos nos livros. Aos funcionários pela ajuda dispensada nos momentos necessários.

Às minhas amigas Inaia, Iana, Vanessa, Mariana e Mayara pelo companheirismo, palavras de incentivo e pela amizade fundamental.

Aos amigos que conheci em Viçosa, por alegrarem meus dias e pelo ombro amigo nos momentos difíceis.

A todas as pessoas que contribuíram para a realização deste trabalho.

A todos meus amigos e amigas que não mencionei, porém, que estão sempre presentes em meu coração e que me apoiaram e incentivaram ao longo do caminho.

BIOGRAFIA

Maria Izabel Costa de Novaes, filha de Aurindo Oliveira de Novaes e Rita de Cassia Costa Silva de Novaes, nasceu em 10 de outubro de 1991, em Tangara da Serra, Estado do Mato Grosso (MT).

Em 2008, ingressou no curso de Agronomia da Universidade Estadual de Montes Claros (UNIMONTES) e graduou-se em julho de 2014.

Em agosto deste mesmo ano, iniciou o curso de Mestrado em Fitopatologia na Universidade Federal de Viçosa (MG).

ÍNDICE

RESUMO

NOVAES, Maria Izabel Costa, M.Sc., Universidade Federal de Viçosa, Julho de 2016. **Aspectos Fisiológicos e Bioquímicos da Soja Pulverizada com Fosfito de Manganês para o Controle de Mofo Branco**. Orientador: Fabrício de Ávila Rodrigues. Coorientadora: Renata Sousa Resende.

Considerando a importância do mofo branco, causado por *Sclerotinia sclerotiorum*, em reduzir a produtividade da soja, novas alternativas para o manejo dessa doença precisam ser investigadas. O presente estudo teve como objetivo determinar o efeito do fosfito de manganês (Mn) no controle do mofo branco em plantas de soja, avaliando o desempenho fotossintético (trocas gasosas e fluorescência da clorofila (Chl) *a*), a participação das enzimas de defesa (*β*-1,3-glucanases (Glu), fenilalanina amônia-liases (PAL) e polifenoloxidases (PPO)) e das enzimas do metabolismo antioxidativo (superóxido dismutase (SOD), catalase (CAT), peroxidase (POX) e ascorbato peroxidase (APX)) e as concentrações de peróxido de hidrogénio (H_2O_2), do superóxido (O_2^-) e de malondialdeído (MDA). A severidade de mofo branco foi significativamente reduzida nas plantas pulverizadas com o fosfito de Mn, as quais apresentaram uma melhor preservação da funcionalidade do aparelho fotossintético com base nos valores dos parâmetros de trocas gasosas e da fluorescência da Chl *a*. As atividades das enzimas SOD, CAT, POX, APX foram maiores nas plantas não pulverizadas com fosfito de Mn e infectadas por *S. sclerotiorum* em comparação com as plantas pulverizadas com esse produto. As atividades da GLU e da PAL nas plantas inoculadas e pulverizadas com fosfito de Mn foram maiores e contribuíram para reduzir a severidade do mofo branco. Em conclusão, o presente estudo apresenta evidências do potencial do fosfito de Mn no controle do mofo branco nos níveis bioquímico e fisiológico

ABSTRACT

NOVAES, Maria Izabel Costa, M.Sc., Universidade Federal de Viçosa, July, 2016. **Physiological and Biochemical Aspects of Soybean Sprayed with Manganese Phosphite for the White Mold Control.** Advisor: Fabrício de Ávila Rodrigues. Co-Advisor: Renata Sousa Resende.

Considering the importance of white mold, caused by *Sclerotinia sclerotiorum*, to decrease soybean yield, new alternatives for disease control need to be investigated. The present study aimed to determine the potential of the manganese (Mn) phosphite in helping soybean plants to counteract *S. sclerotiorum* by examining the photosynthetic performance (leaf gas exchange and chlorophyll (Chl) *a* fluorescence parameters), the participation of defense enzymes (*β*-1,3-glucanases (GLU), phenylalanine ammonia-lyase (PAL) and polyphenoloxidases (PPO)) as well as those related to the antioxidant metabolism (superoxide dismutase (SOD), catalase (CAT), peroxidase (POX) and ascorbate peroxidase (APX)) and the concentrations of hydrogen peroxide (H_2O_2), superoxide (O_2^-) and malondialdehyde (MDA). White mold severity was significantly reduced on plants sprayed with Mn phosphite which showed a better preservation of the functionality of the photosynthetic apparatus based on the values of the leaf gas exchange and Chl *a* fluorescence parameters. The SOD, CAT, POX and APX activities increased for inoculated plants non-sprayed with Mn phosphite in comparison to inoculated plants sprayed with this product. The GLU and PAL activities for inoculated plants sprayed with Mn phosphite were greater and contributed to reduce the white mold severity. In conclusion, the present study brings novel evidence of the potential of Mn phosphite to control white mold at both biochemical and physiological levels.

INTRODUCTION

White mold, caused by *Sclerotinia sclerotiorum* (Lib.) de Bary, is one the most important diseases affecting soybean (*Glycine max* (L.) Merrill) production worldwide (Hegedus and Rimmer, 2005). Symptoms of white mold begins as water-soaked lesions displaying intense white cottony fungal mycelium on their surface at the aerial organs of soybean at any growth stage especially under high relative humidity (Heffer Link and Johnson, 2007). High intensity of white mold can destroy the tissues of soybean plant and results also in wilting, bleaching and plant death (Heffer Link and Johnson, 2007; Mueller *et al*., 2015). At advanced stages of disease development, sclerotia are formed from the fungal cottony mycelium, which can survive in the soil and in plant debris for many years (Heffer Link and Johnson, 2007; Mueller *et al*., 2015; Matsuo *et al*., 2015).

White mold control has been difficult because cultivars with high levels of resistance are not available to growers (Boland and Hall, 1987; Yang *et al*., 1999; Kim and Diers, 2014; Mueller *et al*., 2015). The application of fungicides from several different chemical classes is not always effective in reducing disease intensity (Mueller *et al*., 2002) and *S. sclerotiorum* isolates from common bean that are resistant to thiophanate methyl (benzimidazole) fungicide have been identified (Lehner *et al*., 2015). Therefore, cultural methods such as crop rotation, tillage, wide row spacing, planting date and weed control have been used to limit the yield losses caused by white mold (Heffer Link and Johnson, 2007; Mueller *et al*., 2015).

Considering the importance of white mold to decrease soybean yield, new alternatives for disease management need to be urgently investigated. Induced host resistance has been reported to be effective in the control of diseases caused

by fungi, bacteria, viruses and nematodes on crops of economic importance (Ryals *et al*., 1994; Vallad and Goodman, 2004; Van loon *et al*., 2006). Phosphites are foliar fertilizers composed of a phosporous acid salt that are systemically mobile in the plant and have been shown to be effective in controlling diseases in several economically crops (Smillie *et al*., 1989; Brackmann *et al*., 2004; Peruch and Brunna, 2008; Dianese *et al*., 2009; Nojosa *et al*., 2009; Araujo *et al.,* 2010, 2015; Nascimento *et al*., 2016). Phosphites can act directly by inhibiting fungal mycelial growth and sporulation besides activating host defense mechanisms such as the production of phytoalexins, lignin and ethylene and increasing the activity of phenylalanine ammonia-lyase (Panicker and Gangadharan, 1999; Daniel and Guest, 2006; Dalio *et al*., 2014).

Given the lack of information in the literature regarding the potential of phosphites in white mold control, the present study aimed to determine the potential of the manganese (Mn) phosphite in helping soybean plants to counteract *S. sclerotiorum* infection by examining some plant biochemical and physiological changes associated with the putative Mn phosphite-mediated white mold suppression.

MATERIALS AND METHODS

Plant growth

Five soybean seeds from cultivar M7110IPRO, susceptible to *S. sclerotiorum*, were sown in plastic pots of 2 liters containing 2 kg of Tropstrato® substrate (Vida Verde, Mogi Mirim, São Paulo, Brazil) composed of a mixture of pine bark, peat and expanded vermiculite (1:1:1). Each pot was thinned to three seedlings at 10 days after emergence. Plants were kept in a greenhouse (30 ± 5ºC, 65 ± 5% relative humidity and natural photosynthetically active radiation of 900 ± 5 µmol photons m^{-2} s^{-1}). Plants were fertilized weekly with 100 ml of a modified nutrient solution based on Clark (1975) as follow: 0.8 mM KNO_3, 0.069 mM $NH_4H_2PO_4$, 1 mM NH_4NO_3, 1 mM $Ca(NO_3).4H_2O$, 0.9 mM KCl, 0.6 mM $MgSO_4$ $7H_2O$, 0.5 µM $CuSO_4$ $5H_2O$, 2 µM $ZnSO_4$ $7H_2O$, 19 µM H_3BO_3, 7 µM $MnCl_2$ $4H_2O$, 0.6 µM Na_2MoO_4 $4H_2O$, 60 µM $FeSO_4$ $7H_2O$ and 90 µM disodium ethylenediaminetetraacetic acid (EDTA). Plants were watered deionized water as needed.

Inoculum production, inoculation procedure and treatments

The isolate CMES 1572 of *S. sclerotiorum*, provided by Embrapa Soja (Londrina, Brazil), was used to inoculate the plants. This isolate was preserved in the form of sclerotia. For sclerotia production, carrots were washed, peeled, cut in cubes of approximately 1 × 1 × 1 cm, transferred to Erlenmeyer flasks and autoclaved at 121°C for 20 min (Bae and Knudsen, 2007). Next, two plugs (5 mm in diameter) of potato-dextrose-agar (PDA; 20 g of dextrose, 20 g of agar and 200 g of fresh potato per L of distilled water) obtained from the edge of three-days old colony of *S. sclerotiorum,* were transferred into each Erlenmeyer flasks containing the carrots cubes and incubated in a growth chamber (25 ± 2°C and 12 h

photoperiod) until the sclerotia formation. Sclerotia produced in carrots were placed into glass tubes and kept in refrigerator at 4°C for preservation. For inoculum production, one sclerotia was transferred to each Petri dish containing PDA medium. After 7 days, PDA plugs containing fungal mycelia were transferred to new Petri dishes containing PDA medium, which were kept in a growth chamber (20°C and 12 h photoperiod) for 3 days.

The three leaflets of the third leaf, from the base to the top, of each plant (V3 growth stage, Fehr *et al*., 1971) per replication of each treatment were inoculated with plug (5 mm in diameter) of PDA medium obtained from the edge of three-days old colony of *S. sclerotiorum*. Each PDA plug was placed between the main vein and the edge of the leaflet and gently pressed with the index finger. Inoculated plants were transferred to a plastic mist growth chamber (MGC) inside a greenhouse for the duration of the experiment. The MGC was made of wood (2 m wide, 15 m high, 5 m long) and covered with 100 µm thick transparent plastic. The temperature inside the MGC ranged from 20 ± 2°C (day) to 17 ± 2°C (night). The relative humidity was maintained at 92 ± 3% using a misting system with nozzles (model NEB-100; KGF Co.) that sprayed mist every 30 min above the plant canopy. The relative humidity and temperature were measured with a thermohygrograph (TH-508; Impac). The maximum natural photon flux density at plant canopy height was approximately 900 µmol $m^{-2}s^{-1}$.

At 48 h before inoculation with *S. sclerotiorum*, plants per replication of each treatment were sprayed with water (control treatment), manganese (Mn) phosphite (5 ml L^{-1}, Mn Phytogard® (30% P_2O_5 and 9% Mn), Stoller do Brasil S.A., Cosmopólis, Brazil) and with the fungicide Fluazinam (5 ml L^{-1}; Frowncide® 500 SC, Ishihara Brasil, Sorocaba, Brazil). Plants were sprayed using

a CO_2 pressurized backpack sprayer equipped with a flat fan nozzle (XR 110 02®, Teejet, Glendale Heights, IL, USA) at a 200,000-Pa pressure to give a spray volume of 200 L ha^{-1} (a total of 25 mL per plant).

***In vitro* assays**

The sensitivity of *S. sclerotiorum* to both Mn phosphite and Fluazinam was evaluated *in vitro* using different concentrations of these products as follow: 0, 1.25, 2.5, 5, 10 and 20 ml L^{-1} of PDA medium. These products, at the six concentrations, were incorporated into the PDA medium and then poured into Petri plates (20 ml per plate). After 48 h, one PDA plug (5 mm in diameter), containing fungal mycelia obtained from the edge of a three-days old *S. sclerotiorum* colony, was placed in the central region of each Petri dishes, which were kept in a growth chamber (20°C and 12 h photoperiod). Fungal colony in each Petri dish was measured in two orthogonal directions at 24, 36, 48 and 60 h using a digital paquimeter in order to obtain its diameter.

Assessment of white mold severity

Inoculated leaflets of each plant were collected at 24, 48 and 96 h after inoculation (hai), scanned at 300 dpi resolution and the obtained images were further processed using the software QUANT (Vale *et al*., 2003) to quantify the white mold severity.

Determination of the leaf gas exchange parameters

Leaf gas exchange parameters were determined in one leaflet from the third leaf of each plant (a total of four leaflets per treatment) at 12, 36 and 60 hai. Net carbon assimilation rate (A), stomatal conductance to water vapour (g_s), transpiration rate (E) and internal (C_i) to ambient (C_a) CO_2 concentration ratio (C_i/C_a) were estimated from 09:00 to 12:00 hours (solar time) using a portable

open-system infrared gas analyser (LI-6400; LI-COR Inc.) All measurements were conducted under artificial and saturating photon irradiance (1000 μmol m^{-2} s^{-1} and 400 μmol atmospheric CO_2 mol^{-1}) at the leaf level.

Chlorophyll *a* fluorescence imaging

The Imaging-PAM fluorometer and the Imaging Win software MAXI version (Heinz Walz GmbH, Effeltrich, Germany) were used to obtain the parameters of chlorophyll *a* fluorescence and the images in one leaflet from the third leaf of each plant (a total of four leaflets per treatment) at 12, 24, 48 and 96 hai. Plants were dark-adapted for 1 h and leaflets were placed individually in the CCD ("charge-coupled device") camera to obtain the images at the resolution of 640 × 480 pixels in a support at a distance of 18.5 cm from the CCD camera that was used to capture the chlorophyll *a* fluorescence emission transients. The leaflets were illuminated with a weak modulated measuring beam (0.5 μmol m^{-2} s^{-1}, 100 μs, 1 Hz) to obtain the initial fluorescence (F_0). Saturating white light pulse of 2,400 μmol m^{-2} s^{-1} (10 Hz) was emitted for 0.8 s to determine the maximum fluorescence emission (F_m). Based on these initial measurements, the maximum PS II photochemical efficiency of the dark-adapted leaflets was estimated through the variable-to-maximum chlorophyll *a* fluorescence ratio, $F_v/F_m = [(F_m - F_0)/F_m)]$. Next, the leaflets were exposed to actinic photon irradiance (531 μmol m^{-2} s^{-1}) for 120 s to obtain the steady-state fluorescence yield (F_s), after which a saturating white light pulse (2,400 μmol m^{-2} s^{-1}; 0.8 s) was applied to achieve the light-adapted maximum fluorescence (F_m'). The light-adapted initial fluorescence (F_0') was estimated according to Oxborough and Baker (1997). Based on Kramer *et al*. (2004), the energy that was absorbed by the PS II for the following three yield components for dissipative processes was calculated as follows: the

photochemical yield [Y(II) = (F_m' - F_s)/F_m')], the yield for dissipation by down-regulation [Y(NPQ) = (F_s/F_m') - (F_s/F_m)] and the yield for other non-photochemical (non-regulated) losses [Y(NO*)* = F_s/F_m]. The apparent electron transport rate was calculated as ETR = Y(II) × PPFD × f × α, was estimated according to Baker, 2008.

Determination of the concentration of photosynthetic pigments

Five squared leaflet pieces (1 cm^2) were punched from each leaflet of the third leaf per plant of each replication and treatment at 12, 24, 48 and 96 hai to determine the concentrations of chlorophyll (Chl) *a*, Chl *b* and carotenoids. Leaf samples were immersed in glass tubes containing 5 ml of saturated dimethyl sulfoxide (DMSO) solution (saturated with calcium carbonate ($CaCO_3$), 5 g L^{-1}) and kept in the dark at room temperature for 24 h. The absorbance of the extracts was read at 480, 649.1 and 665.1 nm in spectrophotometer using the $CaCO_3$ saturated solution of DMSO as a blank. Concentrations of Chl *a*, Chl *b* and carotenoids were calculated according to Wellburn (1994).

Biochemical assays

For all biochemical assays, the third leaves, from base to the top, of each plant per replication of each treatment were collected at 12, 24, 48 and 96 hai. Leaf samples were kept in liquid nitrogen during sampling and then stored at -80°C until further analysis.

Determination of the activities of antioxidant enzymes: To determine the activities of superoxide dismutase (SOD), catalase (CAT), peroxidase (POX) and ascorbate peroxidase (APX), a total of 0.2 g of leaf tissue was ground into a fine powder with liquid nitrogen in a mortar and pestle. The fine powder was homogenized in a 2 ml solution containing 50 mM potassium phosphate buffer

(pH 6.8), 0.1 mM EDTA, 1 mM phenylmethyl-sulphonyl fluoride (PMSF) and 2% (w/v) polyvinylpyrrolidone (PVP). The homogenized material was centrifuged at 12000 × *g* at 4°C for 15 min and the supernatant was used for enzyme determination. The SOD activity was determined by measuring its ability to inhibit the photochemical reduction of nitroblue tetrazolium (NBT) as described by Beauchamp and Fridovich (1971) by adding 50 µl of the crude enzyme extract to 1.95 ml of a mixture containing 50 mM potassium phosphate buffer (pH 7.8), 13 mM methionine, 75 µM NBT, 0.1 mM EDTA and 2 µM riboflavin. Samples were exposed to light for 10 min and the production of formazan blue, resulting from the photoreduction of NBT, was measured at 560 nm and the samples kept in the dark for 10 min served as a blank. One unit of SOD was defined as the amount of enzyme necessary to inhibit NBT photoreduction by 50%. Activity of CAT was determined after addition of 50 µl of the crude enzyme extract to 1.95 ml of a reaction mixture containing 50 mM potassium phosphate buffer (pH 7.0) and 20 mM hydrogen peroxide (H_2O_2) (Havir and McHale, 1989). The absorbance was recorded at 240 nm for 1 min. POX activity was assayed by determining the pyrogallol oxidation as proposed by Kar and Mishra (1976). The reaction was started after the addition of 15 µl of the crude enzyme extract to 1.985 ml of a reaction mixture containing 25 mM potassium phosphate (pH 6.8), 20 mM pyrogallol and 20 mM H_2O_2. The activity was determined through the absorbance of colored purpurogallin recorded for 1 min at 420 nm (Chance and Maehly, 1955). APX activity assay was conducted as described by Nakano and Asada (1981). A total of 15 µl of the crude enzyme extract was added to 1.985 ml of a mixture containing 50 mM phosphate buffer (pH 7.0), 1 mM H_2O_2 and 1 mM sodium ascorbate. The rate of ascorbate

oxidation was measured by recording the absorbance at 290 nm for 2 min. Enzyme activity was expressed in a protein-basis whose concentration was determined according to the method of Bradford (1976).

Determination of defense enzymes activities: To determine the activities of *β*-1,3-glucanases (GLU), phenylalanine ammonia-lyase (PAL) and polyphenoloxidase (PPO), a total of 0.2 g of leaf tissue was ground into a fine powder with liquid nitrogen using a mortar and pestle. The fine powder was homogenized in 2 ml of a solution containing 50 mM potassium phosphate buffer (pH 6.8), 1 mM EDTA, 1 mM phenylmethyl-sulfonyl fluoride (PMSF) and 2% (w/v) polyvinylpyrrolidone (PVP). Then, the homogenate was centrifuged at 12000 × *g* for 15 min at 4°C, the supernatant was collected and used to determine the GLU, PAL and PPO activities. The GLU activity was determined according to the method of Lever (1972). First, 20 µl of the crude enzyme extract was added to a reaction mixture containing 50 mM sodium acetate buffer (pH 5.0) and laminarin (1 mg ml^{-1}). Next, the reaction mixture was incubated in a Thermo Mixer (Eppendorf, Hamburg, Germany) at 45°C for 1 h. Then, 500 µl of the reaction mixture was added to 1.5 ml of dinitrosalicylic acid (DNS) and incubated at 100°C for 15 min. The reaction was stopped using an ice bath until the solution reached 25°C. The amount of reducing sugars released was calculated with a calibration curve using glucose (Sigma-Aldrich, São Paulo, Brazil) as a standard and the absorbance was measured at 540 nm (Miller, 1959). A similar procedure was used for the control samples, but the first incubation was excluded. The PAL activity was assayed following the method proposed by Guo *et al*. (2007) with some modifications. First, the reaction was started by adding 100 µl of crude enzyme extract to 0.9 ml of a reaction mixture containing 40 mM sodium borate

buffer (pH 8.8) and 20 mM L-phenylalanine. The reaction mixture was incubated at 30°C for 1 h. For the control samples, the extract was replaced by borate buffer. The reaction was stopped by adding 50 µl of 6 N HCl. The absorbance of the trans-cinnamic acid derivatives was recorded at 290 nm. (Zucker, 1965). PPO activity was assayed following the colorimetric determination of pyrogallol oxidation according to the method of Kar and Mishra (1976) with some modifications. The reaction was started after the addition of 15 µl of the crude enzyme extract to 985 µl of a reaction mixture containing 25 mM potassium phosphate buffer (pH 6.8) and 20 mM pyrogallol. Immediately after the reaction was initiated, the absorbance was determined at 420 nm for 1 min at 25°C.

Determination of malondialdehyde (MDA) concentration: Oxidative damage in the leaf cells was assessed based on lipid peroxidation and expressed as equivalents of MDA according to Cakmak and Horst (1991). A total of 100 mg of leaf tissue was ground into a fine powder using a mortar and pestle with liquid nitrogen and homogenized in 2 ml of 0.1% (w/v) trichloroacetic acid (TCA) solution in an ice bath and the homogenate was centrifuged at 12000 × *g* for 15 min at 4°C. After centrifugation, 0.5 ml of the supernatant was added to 1.5 ml of TBA solution (0.5% in 20% TCA) and held for 30 min in a boiling water bath at 95°C. After this period, the reaction was stopped in an ice bath. The samples were centrifuged at 9000 × *g* for 10 min and the absorbance of the supernatant was read at 532 nm and discounting the non-specific absorbance at 600 nm. The MDA concentration was calculated using the absorption coefficient of 155 mM^{-1} cm^{-1} (Heath and Packer, 1968).

Determination of superoxide (O_2^-) concentration: A total of 0.2 g of leaf tissue was ground into a fine powder in a mortar and pestle with liquid nitrogen. The

fine powder was homogenized in an ice bath in 2 ml of a solution containing 100 mM sodium phosphate buffer (pH 7.2) and 1 mM sodium diethyl dithiocarbamate. The homogenate was centrifuged at 22000 × *g* for 20 min at 4°C. After centrifugation, 0.1 ml of the supernatant was reacted with 1.9 ml of a solution containing 100 mM sodium phosphate buffer (pH 7.2), 1 mM diethyl sodium diethyldithiocarbamate and 0.25 mM p-nitrotetrazolium blue. The O_2^- concentration was determined by subtracting the absorbance of the final product from the initial absorbance at 540 nm (Chaitanya and Naithani, 1994).

Determination of hydrogen peroxide (H_2O_2) concentration: A total of 0.2 g of leaf tissue was ground into a fine powder in liquid nitrogen and homogenized in 2 ml of a mixture containing 50 mM potassium phosphate buffer (pH 6.5) and 1 mM hydroxylamine. The homogenate was centrifuged at 10000 × *g* for 15 min at 4°C (Kuo and Kao, 2003) and the supernatant was used as the crude extract. A total of 100 µl of the supernatant was then added to a reaction mixture containing 100 µM ferric ammonium sulphate ($FeNH_4[SO_4]$), 25 mM sulphuric acid, 250 µM xylenol orange and 100 mM sorbitol in a final volume of 2 ml (Gay and Gebicki, 2000). After 30 min of dark incubation at room temperature, the absorbance of the samples was determined at 560 nm. The sample blanks were prepared under the same conditions and subtracted from the samples. A standard absorbance curve for H_2O_2 (Sigma-Aldrich, São Paulo, Brazil) was used to determine the H_2O_2 concentration.

Histochemical detection of H_2O_2 in the leaflet tissue

One squared leaflet piece (5 cm^2) was punched from each leaflet of the third leaf per plant of each replication and treatment at 96 hai, incubated in 3,3-diaminobenzidine solution (pH 5.5; 1 mg ml^{-1}) in the dark at room temperature for

20 h (Christensen *et al*., 1997). Thereafter, leaflet pieces were boiled in alcohol (96%) for 10 min and scanned at 600 dpi resolution after cooling.

Experimental design and data analysis

A 3 × 2 factorial experiment, consisting of three products [water (control treatment), Mn phosphite and Fluazinam] and non-inoculated or inoculated plants, was arranged in a completely randomized design with four replications. Each replication corresponded to a plastic pot containing three plants. Experiments were repeated once.

All variables were subjected to analysis of variance (ANOVA) and means were compared by Tukey's test ($P \leq 0.05$) using SAS software (SAS Institute Inc., Cary, NC). For withe mold severity and leaf gas exchange measurements, the ANOVA was considered to be a 3 × 2 × 3 factorial experiment, consisting of three products, non-inoculated and inoculated plants and three evaluation times. For the chlorophyll *a* fluorescence parameters, concentration of photosynthetic pigments and biochemical assays, ANOVA was considered to be a 3 × 2 × 4 factorial experiment, consisting of three products, non-inoculated and inoculated plants and four evaluation times.

RESULTS

White mold symptoms, disease severity and lesion area

Water soaked lesions on the leaflets of plants from the control and Mn phosphite treatments were first noticed at 24, whereas no disease symptoms were noticed on plants sprayed with Fluazinam regardless of the sampling time (Fig. 1A, E and G-I). At 48 hai, large lesions showing intense necrosis developed on the leaflets of plants from the control treatment (Fig. 1B-C) in contrast to those observed on the leaflets of plants from the Mn phosphite treatment (Fig. 1E-F). Symptoms of wilting were noticed on the leaflets of plants from the control treatment at 96 hai (Fig. 1C).

The factors Products (P) and (Sampling Time) ST as well as the interaction P × ST were significant for both white mold severity and lesion area (Table 1). White mold severity was significantly reduced by 36 and 86% in the leaflets of plants sprayed with Mn phosphite in comparison to plants from the control treatment at 48 and 96 hai, respectively (Fig. 1J). Fluazinam completely prevented disease development (Fig. 1J and K) Reductions of 60, 61 and 90% in lesion area were recorded in the leaflets of plants sprayed with Mn phosphite in comparison to plants from the control treatment at 24, 48 and 96 hai, respectively (Fig. 1K).

In vitro inhibition of mycelial growth

Inhibition of mycelial growth started at 1.25ml L^{-1} of Mn phosphite and reached 48% of inhibition *S. sclerotiorum* mycelial. The 100% of the inhibition of mycelial growth began at 10ml L^{-1} of Mn phosphite. The EC_{50} value was calculated as 0.913ml L^{-1} (Fig. 2). Fluazinam completely inhibited the mycelium growth on all concentrations evaluated on *in vitro* test.

Leaf gas exchange parameters

The factors P, Plant Inoculation (PI) and ST as well as their interactions were significant for the four leaf gas exchange parameters (Table 1). For the non-inoculated plants, there was no significant effect of the treatments on A, g_s, C_i/C_a and E regardless of the sampling time (Fig. 3A, C, E and G) and neither for the inoculated plants at 12 hai (Fig. 3B, D, F and H). For inoculated plants sprayed with Mn phosphite, the values for A, g_s and E were significantly higher by 45 and 216%, by 43 and 140% and by 57 and 214% at 36 and 60 hai, respectively, in comparison to inoculated plants from the control treatment. The values for A, g_s and E were significantly higher for inoculated plants sprayed with Fluazinam by 102 and 40%, by 143 and 70%, by 133 and 48% at 36 hai and by 663 and 141%, 560 and 175% and by 590 and 120% at 60 hai, respectively in comparison to inoculated plants from the control and Mn phosphite treatments, respectively (Fig. 3B, D and H). The values for C_i/C_a were significantly lower by 14 and 22% at 36 hai and by 22 and 33% at 60 hai, respectively, for inoculated plants sprayed with Mn phosphite and Fluazinam in comparison to inoculated plants from the control treatment. The values for C_i/C_a were significantly lower by 13% for plants sprayed with Fluazinam than for plants sprayed with Mn phosphite at 60 hai (Fig. 3F). For inoculated plants of the control treatment, there were significant decreases of 52 and 87% for A, of 58 and 84% for g_s and 59 and 84% for E at 36 and 60 hai, respectively, in comparison to their non-inoculated counterparts. For plants sprayed with Mn phosphite, *S. sclerotiorum* infection significantly reduced A, g_s and E by 27, 38 and 61% at 36 hai and by 58, 61 and 54% at 60 hai, respectively (Fig. 3A, B, C, D, G and H). Significant increases of 22 and 30% for C_i/C_a at 36 and 60 hai, respectively, occurred for inoculated plants from the control treatment in comparison to their non-inoculated counterparts. At 60 hai,

C_i/C_a significantly increased by 14% for inoculated plants sprayed with Mn phosphite in comparison to their non-inoculated counterparts (Fig. 3E and F).

Chl *a* fluorescence parameters

Images of chlorophyll *a* fluorescence on the leaflets obtained from non-inoculated plants did not show difference among the treatments in terms of color patterns for the parameters F_v/F_m, Y(II), Y(NPQ), Y(NO) and ETR (Fig. 4). For inoculated plants from the control treatment, alterations in the images of Chl *a* fluorescence parameters were already evident at 24 hai. Disease development was accompanied by the progressive loss of photosynthetic capacity as indicated by the black areas in the leaflets of plants from the control treatment at 48 and 96 hai (Fig. 4). For inoculated plants sprayed with Mn phosphite, alterations in the images of Chl *a* fluorescence parameters were evident only at 48 hai. There were small black areas in the leaflets of plants and a progressive loss of photosynthetic capacity was observed at 96 hai, but such alterations in the images of Chl *a* fluorescence parameters were greatly low when compared to the leaflets of plants from the control treatment (Fig. 4). For inoculated plants sprayed Fluazinam, alteration in the images of Chl *a* fluorescence was not evident regardless of the sampling time (Fig. 4).

The factors P, PI and ST as well as their interactions were significant for all Chl *a* fluorescence parameters (Table 1). For the non-inoculated plants, there was no significant effect of the treatments on the parameters F_v/F_m, Y(II), Y(NPQ), Y(NO) and ETR regardless of the sampling time (Fig. 5A, C, E, G and I). Indeed, there was no significant effect of the treatments on the five Chl *a* fluorescence parameters for the inoculated plants at 12 hai and for Y(NPQ) at 24 hai (Fig. 5B, D, F, H and J). For inoculated plants sprayed with Mn phosphite or Fluazinam, the

values for F_v/F_m, Y(II) and ETR were significantly higher from 24 hai onwards and of Y(NPQ) from 48 hai onwards in comparison to those recorded for inoculated plants from the control treatment (Fig. 5B, D, F and J). Conversely, Y(NO) was significantly higher from 24 hai onwards for plants from the control treatment and from 48 hai onwards for plants from the Mn phosphite treatment in comparison to plants sprayed with Fluazinam (Fig. 5H). Values that were significantly higher by 41 and 150% for F_v/F_m, by 19 and 205% for Y(II) and by 28 and 208% for ETR at 48 and 96 hai, respectively, and by 43% for Y(NPQ) at 96 hai, were recorded for inoculated plants sprayed with Fluazinam in comparison to inoculated plants sprayed with Mn phosphite (Fig. 5B, D, F and J). Y(NO) was significantly lower by 58, 49 and 30% for plants from the Mn phosphite treatment and by 50, 59 and 64% for plants sprayed with Fluazinam at 24, 48 and 96 hai, respectively, in comparison to inoculated plants from the control treatment. Inoculated plants sprayed with Fluazinam showed values of Y(NO) that were significantly lower by 19 and 49% at 48 and 96 hai, respectively, in comparison to inoculated plants sprayed with Mn phosphite (Fig. 5H). Significant decreases of 52, 76 and 92% for F_v/F_m, of 85, 100 and 100% for Y(II) and of 85, 100 and 100% for ETR at 24, 48 and 96 hai, respectively, and of 42 and 100% for Y(NPQ) at 48 and 96 hai, respectively, were recorded for the inoculated plants from the control treatment in comparison to their non-inoculated counterparts (Fig. 5A-F, I and J). For plants sprayed with Mn phosphite, *S. sclerotiorum* infection significantly decreased F_v/F_m by 28 and 60%, Y(NPQ) by 20 and 41% and ETR by 26 and 70% at 48 and 96 hai, respectively, in comparison to their non-inoculated counterparts (Fig. 5A, B, E, F, I and J). For inoculated plants sprayed with Mn phosphite, Y(II) significantly decreased by 66% at 96 hai, in comparison

to their non-inoculated counterparts (Fig. 5C and D). Significant increases of 105, 167 and 194% for Y(NO) at 24, 48 and 96 hai, respectively, for inoculated plants from the control treatment and of 30 and 112% at 48 and 96 hai, respectively, for inoculated plants from the Mn phosphite treatment were observed in comparison to the non-inoculated plants (Fig. 5G and H).

Concentration of photosynthetic pigments

The factors P, PI and ST were significant for the concentrations of Chl *a*+*b* and carotenoids as well as some of the 2-way and 3-way interactions (Table 1). For the non-inoculated plants, the concentrations of Chl *a*+*b* and carotenoids (Fig. 6A and C) were not influenced by the treatments regardless of the sampling time and neither for the inoculated plants (Fig. 6B and D) at 12, 24 and 48 hai. At 96 hai, the concentrations of Chl *a*+*b* and carotenoids were significantly higher by 33 and 31%, respectively, for inoculated plants sprayed with Mn phosphite in comparison to inoculated plants from the control treatment (Fig. 6B and D). For inoculated plants sprayed with Fluazinam, the concentrations of Chl *a*+*b* and carotenoids were significantly higher by 131 and 73% and by 74 and 33% in comparison to inoculated plants from the control and Mn phosphite treatments (Fig. 6B and D), respectively, at 96 hai. *S. sclerotiorum* infection significantly decreased the concentrations of Chl *a*+*b* and carotenoids by 51 and 43% for plants from the control treatment and by 38 and 25% for plants from the Mn phosphite treatment (Fig. 6A-D).

Antioxidant enzymes

The factors P, PI and ST as well as their interactions were significant for the activities of SOD, CAT and POX (Table 1). The factors PI and ST and the interaction PI × ST was significant for APX activity (Table 1). For non-inoculated

plants, there was no significant effect of the treatments on the activities of SOD, CAT, POX and APX regardless of the sampling time (Fig. 7A, C, E and G) and neither for the inoculated plants at 12, 24 and 48 hai (Fig. 7B, D, F and H). For inoculated plants, the SOD, CAT and POX activities were significantly lower by 19, 23 and 40% at 96 hai for plants from the Mn phosphite treatment in comparison to plants from the control treatment. Inoculated plants sprayed with Fluazinam showed activities of SOD, CAT, POX and APX that were significantly lower by 41, 50, 64 and 26%, respectively, at 96 hai, in comparison to the inoculated plants from the control treatment and by 27, 34, 41 and 29% in comparison to inoculated plants sprayed with Mn phosphite (Fig. 7B, D, F, and H). For inoculated plants from the control treatment, there were significant increases of 73, 82, 217 and 55% for SOD, CAT, POX and APX, respectively, at 96 hai in comparison to non-inoculated plants (Fig. 7A-H). There were significant increases of 41, 58, 59 and 65% for SOD, CAT, POX and APX activities, respectively, at 96 hai, for inoculated plants sprayed with Mn phosphite in comparison to non-inoculated ones (Fig. 7A-H).

Defense enzymes

The factors P, PI and ST as well as their interactions were significant for the activities of GLU, PAL and PPO (Table 1). For the non-inoculated plants, there was no significant effect of the treatments on the activities of GLU, PAL and PPO irrespective of the sampling time (Fig. 7I, K and M) and neither for the inoculated plants at 12, 24 and 48 hai (Fig. 7J, L and N). Activities of GLU and PAL for the inoculated plants sprayed with Mn phosphite were significantly higher by 47% and 114%, respectively, at 96 hai in comparison to the inoculated plants from control treatment (Fig. 7J and L). PPO activity was significantly lower by 67% for

the inoculated plants sprayed with Mn phosphite in comparison to the inoculated plants from the control treatment (Fig. 7N). Inoculated plants sprayed with Fluazinam showed activities of GLU and PPO that were significantly lower by 40 and 65%, respectively, in comparison to the inoculated plants from the control treatment and by 59 and 65%, respectively, in comparison to the inoculated plants sprayed with Mn phosphite at 96 hai (Fig. 7J and N). GLU and PPO activities significantly increased by 67 and 202%, respectively, for the inoculated plants from control treatment in comparison to the non-inoculated ones (Fig. 7I, J, M and N) and the GLU and PAL activities significantly increased by 144 and 134%, respectively, for the Mn phosphite treatment at 96 hai, in comparison to the non-inoculated ones (Fig. 7I-L).

Concentrations of O_2, H_2O_2 and MDA

The factors P and some of the 2-way and 3-way interactions were significant for the O_2^- concentration (Table 1). The factors P and ST and some of the 2-way interactions were significant for the H_2O_2 concentration (Table 1). The factors P, PI and ST as well as their interactions were significant for the MDA concentration (Table 1). For the non-inoculated plants, there was no significant effect of the treatments on the concentrations of O_2^-, H_2O_2 and MDA regardless of the sampling time (Fig. 8G, I and K). In addition, there was no significant effect of the treatments on the O_2^-, H_2O_2 and MDA concentrations for the inoculated plants at 12 and 24 hai and for the O_2^- concentration at 48 hai (Fig. 8H, J and L). The concentrations of H_2O_2 were significantly lower by 16 and 19% at 48 and 96 hai, respectively, and the concentrations of O_2^- and MDA by 41 and 27%, respectively, at 96 hai for the inoculated plants sprayed with Mn phosphite in comparison to the inoculated plants from the control treatment (Fig. 8H, J, and L).

Inoculated plants sprayed with Fluazinam showed concentrations of H_2O_2 and MDA that were significantly lower by 32 and 41% respectively, in comparison to the inoculated plants from the control treatment and by 16 and 34%, respectively, in comparison to the inoculated plants sprayed with Mn phosphite at 48 hai (Fig. 8J and L). Inoculated plants sprayed with Fluazinam showed concentrations of O_2^-, H_2O_2 and MDA that were significantly lower by 47, 45 and 58% at 96 hai, respectively, in comparison to the inoculated plants from the control treatment (Fig. 8H, J, and L). Concentrations of H_2O_2 and MDA at 96 hai were significantly lower by 34 and 42% for the inoculated plants sprayed with Fluazinam in comparison to inoculated plants sprayed with Mn phosphite (Fig. 8J and L). There were significant increases of 113% for O_2^- concentration at 96 hai, of 14 and 44% for H_2O_2 concentration and of 34% and 122% for MDA concentration at 48 and 96 hai, respectively, for the inoculated plants from the control treatment in comparison to the non-inoculated ones (Fig. 8G-L). Concentrations of H_2O_2 and MDA were significantly higher by 23 and 60%, respectively, for inoculated plants sprayed with Mn phosphite relative to their non-inoculated counterparts at 96 hai (Fig. 8I-L).

Histochemical detection of H_2O_2

The histochemical analysis performed in the present study, show the non-inoculated plants, there was no significant effect of the treatments on the accumulation of H_2O_2. Inoculated plants with *S. sclerotiorum* resulted in an extensive production of H_2O_2. The accumulation of H_2O_2 were lower for the inoculated plants sprayed with Mn phosphite in comparison to the inoculated plants from the control treatment. Fluazinam completely inhibited pathogen-induced H_2O_2 accumulation.

DISCUSSION

Phosphites have been shown to reduce diseases' intensity in many crops of economic importance, including brown spot on rice (Nascimento *et al*., 2016) Ceratocystis wilt on mango (Araujo *et al.,* 2015), downy mildew on grape (Peruch and Brunna, 2008), foot rot on papaya (Dianese *et al*., 2009), Glomerella leaf spot on apple (Araujo *et al.*, 2012), Phoma leaf spot on coffee (Nojosa *et al*., 2009) powdery mildew on cucumber (Reuveni *et al.*, 1995) and scab on pecan (Bock *et al.*, 2013). However, there are few evidences at the biochemical and physiological levels uncovering mechanisms underlying phophiste-mediated plant disease control. To our knowledge, this study provide novel insights regarding the role of Mn phosphite in white mold control on soybean.

White mold severity and lesion area were found to be decreased in Mn phosphite-sprayed soybean leaflets, indicating its potential to constraint *S. sclerotiorum* infection. Phosphites can inhibit fungal mycelial growth directly or act indirectly by activating host defense mechanisms (Mersha *et al*., 2012, Dalio *et al*., 2014). In soybean, Mn phosphite was demonstrated to be fastly translocable in both xylem and phloem and it was able to reduce charcoal rot (*Macrophomina phaseolina*) symptoms, which was ascribed to its ability to induce defense responses (Simoneti *et al.*, 2015). Both direct and indirect actions of phosphite were found to be operating in constrained infection of *Fagus sylvatica* plants by *Phytophthora plurivora* (Dalio *et al*., 2014). No white mold symptoms were noticed on leaflets of soybeans plants sprayed with the fungicide Fluazinam. Accordingly, Fluazinam is known to directly act on *S. sclerotiorum* mycelium at the plant leaf surface, inhibiting fungal growth and further penetration into the host tissue (Sumida *et al*., 2015).

It has been demonstrated that phosphites have a fungistatic effect on many pathogens (Araujo *et al*., 2010; Dalio *et al*., 2014; Spolti *et al*., 2015). *In vitro* test showed that Mn phosphite in concentrations compatible to that used *in vivo* conditions inhibited the mycelial growth of *S. sclerotiorum*. Mycelial growth was inhibited in a dose-dependent manner, with higher concentrations of phosphite conferring higher inhibition and Ec_{50} value of 0.913 ml L^{-1}. Therefore, a direct action on *S. sclerotiorum* mycelium is thought to be involved, at least partially, in suppression of white mold symptoms observed in Mn phosphite-treated soybean leaflets.

Soybean photosynthesis was found to be dramatically depressed in response to *S. sclerotiorum* infection, consistent with observations made for other pathosystems (Bu *et al*., 2009, Yang *et al*., 2014, Bermúdez-Cardona *et al*., 2015). The progressive decreases in *A* observed in *S. sclerotiorum*-infected soybean leaflets may be explained by the secretion of the non-host selective toxin named oxalic acid that is able to completely destroy the leaf cells compromising, therefore, water and nutrients translocation throughout the leaf tissue (Yoshii, 1937; Bateman and Beer, 1965). Yang *et al*. (2014) reported that the oxalic acid was of pivotal importance for the establishment of *S. sclerotiorum* infection on tobacco leaves resulting, therefore, in lower photosynthetic activity. Decreases in both g_s and *E* caused by *S. sclerotiorum* infection were associated with stomatal closure, probably because of high production of reactive oxygen species (ROS) and the deregulation of guard cells. Some reports have suggested that *S. sclerotiorum*-secreted oxalate deregulates host guard cells (Guimaraes and Stotz, 2004) and also it mediates antagonistic interactions between abscisic acid and other phytohormones (Guo and Stotz, 2010). Despite the reduced stomatal

aperture, which could have reduced CO_2 influx, a progressive increase in the C_i/C_a values was observed as the white mold symptoms developed. Therefore, decreases in *A* were most likely associated to biochemical constraints or diffusive limitations to photosynthesis at the mesophyll level rather than to lower g_s. Similar findings have been reported for rice-*Bipolaris oryzae* (Debona *et al.*, 2016), maize-*Sternocapella. macrospora* (Bermúdez-Cardona *et al*., 2015) and wheat-*Pyricularia oryzae* interactions (Debona *et al*., 2014).

The reduced symptoms of white mold recorded in Mn phosphite-sprayed soybean leaflets was associated with greater values of *A*, g_s and *E* compared to the non-sprayed leaflets, suggesting that Mn phosphite was able to attenuate the *S. sclerotiorum*-induced physiological impairments. . In addition, we found that Fluazinam, by completely inhibiting *S. sclerotiorum* infection, deny all of pathogen-induced physiological impairments. Consistent with our findings, UV-B-induced damage to the photosynthetic machinery were found to be prevented by potassium phosphite (Oyaburo *et al*., 2015). Similarly, while *P. plurivora* infection dramatically depressed *A*, water uptake and RuBisCO activity in non-treated *F. sylvatica* plants, phosphite treatment prevented all of the pathogen-induced physiological dysfunctions (Dalio *et al*., 2014).

The photochemical performance of *S. sclerotiorum*-infected soybean leaflets was progressively reduced as the white mold severity increased. Indeed, infected soybean leaflets displayed clear adjustments in light capture and dissipation, as evidenced by changes in the Chl *a* fluorescence parameters. The decrease in the maximum photochemical efficiency of PSII, based on the F_v/F_m values, indicated the occurrence of photoinhibition on photosynthetic apparatus as a consequence of *S. sclerotiorum* infection. Additionally, the reductions in Y(II), which is a relative

measure of the PSII performance, suggested that the energy absorbed by photosynthetic pigments of *S. sclerotiorum*-infected leaflets was not directed to the photochemical process, probably stemmed from pathogen-induced photooxidative damage. The reductions in Y(NPQ) caused by *S. sclerotiorum* infection may be associated with low plant capacity to regulate thermal dissipation, which resulted in photosynthetic damage. The increased photooxidative damage in *S.sclerotiorum*-infected soybean leaflets may also be depicted from the progressive increases in Y(NO), which suggest that the regulation mechanisms of protection become ineffective (Klughammer and Schreiber, 2008), culminating in dramatic decreases in ETR at advanced stages of *S. sclerotiorum* infection, which can be attributed to the lytic enzymes and non-selective toxins that disrupt the electron transport chain in the thylakoid membrane. According to Yang *et al*. (2014), the activity of PSII on tobacco leaves was significantly compromised during *S. sclerotiorum* infection, fact that was ascribed to damage to the reaction centers and the acceptor side of photosystem II (PSII) by *S. sclerotiorum*-secreted oxalate, thereby causing photochemical dysfunctions. However, photochemical dysfunctions were greatly reduced in Mn phosphite-sprayed leaflets and completely prevented in Fluazinam-sprayed ones, indicating that their ability to capture and exploit light energy was not as compromised as to the non-sprayed leaflets.

The concentration of photosynthetic pigments was negatively affected by *S. sclerotiorum* infection, but higher decreases were reported for the non-sprayed leaflets than for the Mn phosphite- or Fluazinam-sprayed ones. Decreases on the concentration of photosynthetic pigments could be associated with the action of oxalic acid that shifts pH as well as with cell wall degrading enzymes, such as the

polygalacturonases, secreted by *S. sclerotiorum* as the white mold develops (Bateman and Beer, 1965). In addition, oxalic acid is known to cause chloroplasts degeneration (Tariq and Jefferies, 1985). Decreases on total chlorophyll concentration has been also reported on mint leaves infected by *S. sclerotiorum* (Perveen *et al*., 2010).

ROS production is a common response of plants against pathogens' infection (Doke *et al*., 1996). The oxidative burst can be suppressed in the beginning of *S. sclerotiorum* infection, whereas it can increase later due to the intense secretion of oxalic acid by the fungus (Willian *et al*., 2011; Zhou *et al*., 2013). The antioxidant defense system on plants co-evolved with the aerobic metabolism to counteract the oxidative damage caused by the ROS (Malencic *et al*., 2010). SOD is a key enzyme in protecting plant cells against the deleterious effect of ROS by converting O_2^- to H_2O_2 and O_2 (Apel *et al*., 2004; Hao *et al*., 2011), whereas CAT, POX and APX play a pivotal role in H_2O_2 detoxifying. In the present study, all of the studied antioxidant enzymes had their activities increased in *S. sclerotiorum*-infected leaflets mainly in non-sprayed ones. However, it seems such activation of antioxidant system was not sufficient to prevent oxidative damage, as high concentrations of $O_2^-$and H_2O_2 were recorded. The Mn phosphite-sprayed-inoculated leaflets displayed lower activities of SOD, CAT and POX in comparison to their non-sprayed counterparts. This results associated with less severity of white mold suggest the potential of this product to protect in limiting pathogen-induced O_2^- and H_2O_2 generation, which in turn, can reduce the cellular damage.

The increase in the concentrations of both O_2^- and H_2O_2 contributed to the higher concentration of the cell damage indicator MDA as a result of *S.*

sclerotiorum infection. However, Mn phosphite was found to greatly limit pathogen-induced cellular damage. Lipid peroxidation in cell membrane resulting from oxidative stress promoted by pathogens infection can eventually lead to release of organelles and electrolytes (Mandal *et al*., 2008). In cucumber, *S. sclerotiorum* was shown to increase MDA content, indicating the fungus can damage cell membrane (Bu *et al*., 2009). Although histochemical analysis performed in the present study confirmed that *S. sclerotiorum* resulted in an extensive production of H_2O_2, mainly in symptomatic tissue, Mn phosphite constrained the area where H_2O_2 was generated, and Fluazinam completely inhibited pathogen-induced H_2O_2 accumulation.

Plants are able to activate a wide range of defense responses to counteract pathogens' infection. GLU, enzyme that catalyzes the hydrolysis of fungal cell wall components may also release elicitors of host defense responses (Keen and Yoshikawa 1983). PAL, a major enzyme in the phenylpropanoid pathway, is responsible for the production of different phenolics and some of them exhibit antimicrobial action against fungal pathogens (Schuster and Rétey, 1995). In the present study, activities of GLU and PAL were higher in inoculated leaflets sprayed with Mn phosphite than in their non-sprayed counterparts at 96 hai, suggesting the potential of this product to induce soybean resistance against white mold. Accordingly, phosphite treatment of potato leaves increased GLU activity upon *Phytophthora infestans* infection (Lobato *et al.*, 2008, 2011). PAL activity was also increased phosphite-treated rapevine plants, fact that was associated with the reduced symptoms of downy mildew observed in such plants (Pinto *et al.*, 2012). Our results suggest that Mn phosphite could prime soybean plants for enhanced defense against *S. sclerotiorum*. By definition, priming occurs when a

plant, prior to exposure by some compound or microorganism, exhibits an augmented defense response under pathogen attack (Conrath *et al*., 2002). According to Machinandiarena *et al*. (2012), phosphite increased potato resistance to *P. infestans* due to a high expression of genes involved in the systemic acquired resistance. Priming was also found to be involved in *P. plurivora* control in *F. sylvatica* by phopshite (Dalio *et al.*, 2014).

In conclusion, the present study brings novel evidence of the potential of Mn phosphite to control white mold in soybean. While *S. sclerotiorum* dramatically impairs photosynthetic performance soybean and induces cellular damage, Mn phosphite greatly constraints such dysfunctions. There is still no conclusive explanation regarding the mode of action of phosphite and its potential targets in plants. From the results obtained in this study, we conclude that Mn phosphite might act in a dual way, by a direct action on *S. sclerotiorum* or activating soybean defense responses, but the former mechanism it appears to play a major role in white mold control.

REFERENCES

Apel K, Hirt H, 2004. Reactive oxygen species: Metabolism, oxidative stress, and signal transduction. *Annual Review of Plant Biology* 55, 373-399.

Araujo L, Valdebenito-Sanhueza RM, Stadnik MJ, 2010. Avaliação de formulações de fosfito de potássio sobre *Colletotrichum gloeosporioides* in vitro e no controle pós-infeccional da mancha foliar de Glomerella em macieira. *Tropical Plant Pathology* 35, 54-59.

Araujo L, Bispo WMS, Rios VS, Fernandes SA, Rodrigues FA, 2015. Induction of the phenylpropanoid pathway by acibenzolar-s-methyl and potassium phospite increases mango resistance to *Ceratocystis fimbriata* infection. *Plant Disease* 99, 447-459.

Bae YS, Knudsen GR, 2007. Effect of sclerotial distribution pattern of *Sclerotinia sclerotiorum* on biocontrol efficacy of *Trichoderma harzianum*. *Applied Soil Ecology* 35, 21-24.

Baker NR, 2008. Chlorophyll fluorescence: A probe of photosynthesis in vivo. *Annual Review of Plant Biology* 59, 89-113.

Bateman DF, Beer SV, 1965. Simultaneous production and synergistic action of oxalic acid and polygalacturonase during pathogenesis by *Sclerotium rolfsii*. *Phytopathology* 55, 204-211.

Beauchamp C, Fridovich I, 1971. Superoxide dismutase; Improved assays and assay applicable to aerylamide gels. *Analytical Biochemistry* 44, 276-287.

Bermúdez-Cardona MB, Wordell Filho JA, Rodrigues FA, 2015. Leaf gas exchange and chlorophyll *a* fluorescence in maize leaves infected with *Stenocarpella macrospora*. *Phytopathology* 105, 26-34.

Boland GJ, Hall R, 1987. Evaluating soybeans cultivars for resistance to *Sclerotinia sclerotiorum* under field conditions. *Plant Disease* 71, 934-936.

Brackmann1 A, Giehl RFH, Sestari I, Steffens CA, 2004. Fosfitos para o controle de podridões pós-colheita em maçãs 'Fuji' durante o armazenamento refrigerado. *Ciência Rural* 34, 1039-1042.

Bradford MN, 1976. A rapid and sensitive method for the quantitation of microgram quantities of protein utilizing the principle of protein-dye binding. *Analytical Biochemistry* 72, 248-254.

Bock CH, Brenneman TB, Hotchkiss MW, Wood BW, 2013 Evaluation of a phosphite fungicide to control pecan scab in the southeastern USA. *Crop Protection* 36,58-64.

Bu JW, Yao G, Gao HY, Jia YJ, Zhang LT, Cheng DD, Wang X, 2009. Inhibition mechanism of photosynthesis in cucumber leaves infected by *Sclerotinia sclerotiorum* (Lib.) de bary. *Acta Phytopathologica Sinica* 39, 613-621.

Cakmak I, Horst WJ, 1991. Effect of aluminum on lipid peroxidation, superoxide dismutase, catalase, and peroxidase activities in root tips of soybean (*Glycine max*). *Physiologia Plantarum* 83, 463-468.

Chaitanya KSK, Naithani SC, 1994. Role of superoxide lipid peroxidation and superoxide 370 dismutase in membrane perturbation during loss of viability in seeds of Shorea robusta 371 Faertn. *New Phytologist* 126, 623-627.

Chance B, Maehley AC, 1955. Assay of catalases and peroxidases. *Methods in Enzymology* 2, 764-775.

Clark RB, 1975. Characterization of phosphates in intact maize roots. *Journal of Agricultural Food Chemistry* 23, 458-460.

Conrath U, Pieterse CMJ, Mauch-Mani B, 2002. Priming in plant-pathogen interactions. *Trends in Plant Science* 7, 210–216.

Dalio RJD, Fleischmann F, Humez M, Osswald W, 2014. Phosphite protects *Fagus sylvatica* seedlings towards *Phytophthora plurivora* via local toxicity, priming and facilitation of pathogen recognition. *Plos One* 9, e87860.

Daniel R, Guest D, 2006. Defense responses induced by potassium phosphonate in *Phytophthora palmivora*-challenged *Arabidopsis thaliana*. *Physiological and Molecular Plant Pathology* 67, 194-201.

Debona D, Rodrigues FA, Rios JA, Nascimento KJT, 2012. Biochemical changes in the leaves of wheat plants infected by *Pyricularia oryzae*. *Phytopathology* 102, 1121-1129.

Debona D, Nascimento KJT, Gomes JGO, Aucique-Pérez CE, Rodrigues FA, 2015. Physiological changes promoted by a strobilurin fungicide in the rice-*Bipolaris oryzae* interaction. *Pesticide Biochemistry and Physiology* 10, 8-16.

Dianese AL, Blum LEB, Dutra JB, Lopes LF, 2009. Aplicação de fosfito de potássio, cálcio ou magnésio para a redução da podridão-do-pé do mamoeiro em casa de vegetação. *Ciência Rural* 29, 2309-2314.

Doke N, Miura Y, Sanchez LM, Park HJ, Noritake T, Yoshioka H, Kawakita K, 1996. The oxidative burst protects plants against pathogen attack: mechanism and role as an emergency signal for plant biodefence. *Gene* 179, 45-51.

Fehr WR, Caviness CE, Burmood DT, Pennington JS, 1971. Stage of development descriptions for soybeans, *Glycine max* (L.) Merrill. *Crop Science* 11, 929-931.

Gay C, Gebicki JM, 2000. A critical evaluation of the effect of sorbitol on the ferric-xylenol orange hydroperoxide assay. *Analytical Biochemistry* 284, 217-220.

Guimarães RL, Stotz HU, 2004. Oxalate production by *Sclerotinia sclerotiorum* deregulates guard cells during infection. *Plant Physiology* 136, 3703-3711.

Guo X, Stotz H, 2010. ABA signaling inhibits oxalate-induced production of reactive oxygen species and protects against *Sclerotinia sclerotiorum* in *Arabidopsis thaliana. European Journal Plant Pathology 128,7–19.*

Guo Y, Liu L, Bi Y, 2007. Use of silicon oxide and sodium silicate for controlling *Trichothecium roseum* postharvest rot in Chine cantaloupe (*Cucumis melo* L.). *International Journal of Food Science & Technology* 42, 1012-1018.

Hao Z, Wang L, Liang J, Thao R, 2011. Expression of defense genes and activities of antioxidant enzymes in rice resistance to rice stripe virus and small brown plant hopper. *Plant Physiology and Biochemistry* 7, 744-751.

Havir EA, MChale NA, 1989. Enhanced – peroxidatic activity in specific catalase isozymes of tobacco, barley, and maize. *Plant Physiology* 91, 812-815.

Heath RL, Packer L, 1968. Photoperoxidation in isolated chloroplast. I Kinetics and stoichometry of fatty acid peroxidation. *Archives of Biochemistry and Biophysics* 125, 189-198.

Heffer Link V, Johnson KB, 2007. White Mold: The Plant Health Instructor. [http://www.apsnet.org/edcenter/intropp/lessons/fungi/ascomycetes/Pages/WhiteMold.aspx]. Acessed 9 June 2016.

Hegedus DD, Rimmer SR, 2005. *Sclerotinia sclerotiorum*: When to be or not to be a pathogen? *Federation of European Microbiological Societies Microbiology Letters* 251, 177-184.

Kar M, Mishra D, 1976. Catalase, peroxidase, and polyphenol oxidase activities during rice leaf senescence. *Plant Physiology* 57, 315-319.

Keen NT, Yoshikawa M, 1983. β-1,3-endoglucanase from soybean releases elicitor active carbohydrates from fungus cell walls. *Plant Physiology* 71, 460-465.

Kim HS, Diers BW, 2014. Inheritance of partial resistance to *Sclerotinia* stem rot in soybean. *Crop Science* 40, 55-61.

Klughammer C, Schreiber U, 2008. Complementary PSII quantum yield calculated from simple fluorescence parameters measured by PAM fluorometry and saturation pulse method. *PAM Application Notes* 1, 27–35.

Kramer DM, Johnson G, Kiirats O, Edwards GE, 2004. New fluorescence parameters for the determination of QA redox state and excitation energy fluxes. *Photosynthesis Research* 79, 209-218.

Kuo MC, Kao CH, 2003. Aluminum effects on lipid peroxidation and antioxidative enzyme activities in rice leaves. *Biologia Plantarum* 46, 149-152.

Lehner MS, Paula Junior TJ, Silva RA, Vieira RF, Carneiro JES, Schnabel G, Mizubuti ESG, 2015. Fungicide sensitivity of *Sclerotinia sclerotiorum*: A thorough assessment using discriminatory dose, ec_{50}, high-resolution melting analysis, and description of new point mutation associated with thiophanate-methyl resistance. *Plant Disease* 99, 1537-1543.

Lever M, 1972. A new reaction for colorimetric determination of carbohydrates. *Analytical Biochemistry* 47, 273-279.

Lobato MC, Olivieri FP, González Altamiranda E, Wolski E, Daleo GR, Caldiz DO, Andreu AB, 2008. Phosphite compounds reduce disease severity in potato seed tubers and foliage. *European Journal of Plant Pathology* 122, 349-358.

Lobato MC, Olivieri FP, Daleo GR, Andreu AB, 2011. Antimicrobial activity of phosphites against different potato pathogens. *Journal of Plant Disease and Protection* 117, 102-109.

Machinandiarena MF, Lobato MC, Feldman ML, Daleo GR, Andreu AB, 2012. Potassium phosphite primes defense responses in potato against *Phytophthora infestans*. *Journal of Plant Physiology* 149, 1417-1424.

Mandal S, Mitra A, Mallick N, 2008. Biochemical characterization of oxidative burst during interaction between *Solanum lycopersicum* and *Fusarium oxysporum* f. sp. *lycopersici*. *Physiological and Molecular Plant Pathology* 72, 56–61.

Matsuo E, Lopes EA, Sediyama T, 2015. Manejo de Doenças. In: Sediyama T, Silva F, Borem A, eds: Soja: Plantio a Colheita: Viçosa, Minas Gerais, Brasil. Editora UFV, pp. 288-309.

Miller GL, 1959. Use of dinitro salicylic acid reagent for determination of reducing sugar. *Analytical Chemistry* 31, 426-428.

Mueller DS, Dorrance AE, Derksen RC, Ozkan E, Kurle JE, Grau CR, Gaska JM, Hartman GL, Bradley CA, Pedersen WL, 2002. Efficacy of fungicides on *Sclerotinia sclerotiorum* and their potential for control of *Sclerotinia* stem rot on soybean. *Plant Disease* 86, 26-31.

Mueller D, Bradley C, Chilvers M, Esker P, Malvick D, Peltier A, Sisson A, Wise K, 2015. White mold: Soybean Disease Management. *Crop Protection Network*, 1005: [http://www.ncsrp.com/pdf_doc/WhiteMold_CPN1005_2015.pdf]. Acessed 10 June 2016.

Nakano Y, Asada K, 1981. Hydrogen peroxidase is scavenged by ascorbate specific peroxidases in spinach chloroplasts. *Plant and Cell Physiology* 22, 867-880.

Nascimento KJT, Araujo L, Resende RS, Schurt DA, Silva WL, Rodrigues FA, 2016. Silicon, acibenzolar-S-methyl and potassium phosphite in the control of brown spot in rice. *Bragantia* 75, 212-221.

Nascimento KJT, Debona D, Silveira PR, Silva, LC, Damatta FM, Rodrigues FA, 2016. Silicon-induced changes in the antioxidant system reduce soybean resistance to frogeye leaf spot. *Journal of Phytopathology* (doi 10.1111/jph.12497).

Nojosa GBA, Resende MLV, Barguil BM, Moraes SRG, Vilas Boas CH, 2009. Efeito de indutores de resistência em cafeeiro contra a mancha de Phoma. *Summa Phytopathologica* 35, 60-62.

Oxborough K, Baker NR, 1997. An instrument capable of imaging chlorophyll *a* fluorescence from intact leaves at very low irradiance and at cellular and subcellular levels of organization. *Plant, Cell & Environment* 20, 1473-1483.

Oyarburo NS, Machinandiarena MF, Feldman ML, Daleo GR, Andreu AB, Oliveira FP, 20015. Potassium phosphite increases tolerance to UV-B in potato. *Plant Physiology and Biochemestry* 88, 1-8.

Panicker S, Gangadharam K, 1999. Controlling downy mildew of maize caused by *Peronosclerospora sorghi* by foliar sprays of phosphonic acid compounds. *Crop Protection* 18, 115-118.

Perveen K, Haseen A, Shukla PK, 2010. Effect of *Sclerotinia sclerotiorum* on the disease development, growth, oil yield and biochemical changes in plants of *Mentha arvensis. Saudi Journal of Biological Sciences* 17, 291-294.

Peruch LAM, Brunna ED, 2008. Relação entre doses de calda bordalesa e de fosfito potássio na intensidade do míldio e na produtividade da videira cv. 'Goethe'. *Ciência Rural* 38, 2413-2418.

Pinto KMS, Nascimento LC, Gomes ECS, Silva HF, Miranda JR, 2012. Efficiency of resistance elicitors in the management of grapevine downy mildew *Plasmopara viticola*: epidemiological, biochemical and economic aspects. *European Journal of Plant Phytopathology* 134, 745-754.

Reuveni M, Agapov V, Reuveni R, 1995. Suppression of cucumber powdery mildew (*Sphaerotheca fuliginea*) by foliar sprays of pbospbate and potassium salts. *Plant Pathology* 44, 31-39.

Ryals J, Uknes S, Wars E, 1994. Systemic acquired resistance. *Plant Physiology* 104, 1109-1112.

Schuster B, Rétey J, 1995. The mechanism of action of phenylalanine ammonia-lyase: The role of prosthetic dehydrolanine. *Proceedings of the National Academy of Science* of *the United States of America* 92, 8433-8437.

Simonetti E, Viso NP, Montecchia M, Zilli C, Balestrasse K, Carmona M, 2015. Evaluation of native bacteria and manganese phosphite for alternative control of charcoal root rot of soybean. *Microbiological Research* 180, 40-48.

Smillie R, Grant BR, Guest D, 1989. The mode of action of phosphite: evidence for both direct and indirect modes of action on three *Phytophthora* spp. in plants. *Phytopathology* 79, 921-926.

Spolti P, Valdebenito-Sanhueza RM, Campos AD, Del Ponte EM, 2015. Modo de ação de fosfitos de potássio no controle da podridão olho de boi em maçã. *Summa Phytopathologica* 41, 42-48.

Sumida CH, Canteri MG, Peitil DC, Tibolla F, Orsini IP, Araujo FA, Chagas DF, Calvos NS, 2015. Chemical and biological control of *Sclerotinia* stem rot in the soybeans crop. *Ciência Rural* 45, 760-766.

Tariq VN, Jeffries P, 1985. Changes occurring in chloroplasts of *Phaseolus* following infection by *Sclerotinia*: A cytochemical study. *Journal of Cell Science* 75, 195-295.

Thordal Christensen H, Zhang Z, Wei Y, Collinge DB, 1997. Subcellular localization of H_2O_2 in plants. H_2O_2 accumulation in papillae and hypersensitive response during the barley-powdery mildew interaction. *Plant Journal* 11, 1187-1194.

Vallad GE, Goodman RM, 2004. Systemic acquired resistance and induced systemic resistance in conventional agriculture. *Crop Science* 44, 1920-1934.

Vale FXR, Fernandes Filho EI, Liberato JR, 2003. A software plant disease severity assessment. In: Close R, Braithwaite M, Havery I, eds. Proceedings of Eighth International Congress of Plant Pathology, Christchurch, New Zealand. Sydney, Australia: *Horticulture Australia*, 107.

Van Loon LC, Rep M, Pieterse CMJ, 2006. Significance of inducible defense-related proteins in infected plants. *Annual Review of Phytopathology* 44, 135-162.

Wellburn AR, 1994. The spectral determination of chlorophylls *a* and *b*, as well as total carotenoids, using various solvents with spectrophotometers of different resolution. *Journal of Plant Physiology* 144, 307-313.

Williams B, Kabbage M, Kim HJ, Britt R, Dickman MB, 2011. Tipping the balance: *Sclerotinia sclerotiorum* secreted oxalic acid suppresses host defenses by manipulating the host redox environment. *Plos Pathogens* 7, e1002107.

Yang XB, Lundeen P, Uphoff MD, 1999. Soybean varietal response and yield loss caused by *Sclerotinia sclerotiorum*. *Plant Disease* 83, 456-461.

Yang C, Zhang Z, Gao H, Liu M, Fan X, 2014. Mechanisms by which the infection of *Sclerotinia sclerotiorum* (Lib.) de Bary affects the photosynthetic performance in tobacco leaves. *BMC Plant biology* 14, 1-11.

Yoshii H, 1937. Pathological studies of rice blast caused by *Pyricularia oryzae*. III Pathohistological observations of diseased plants. *Annals of the Phytopathological Society of Japan* 6, 289-304.

Zhou J, Sun A, Xing D, 2013. Modulation of cellular redox status by thiamine-activated NADPH oxidase confers *Arabidopsis* resistance to *Sclerotinia sclerotiorum. Journal of Experimental Botany* 64, 3261-3272.

Zucker M, 1965. Induction of phenylalanine deaminase by light and its relation to chlorogenic acid synthesis in potato tuber tissue. *Plant Physiology* 40, 779-784.

LIST OF TABLES AND FIGURES

Table 1. Analysis of variance of the effects of products (P), plant inoculation (PI), sampling time (ST) and their interactions for white mold severity (WMS), lesion area (LA), leaf gas exchange parameters (net CO_2 assimilation rate (A), stomatal conductance to water vapor (g_s), internal to ambient CO_2 concentration ratio (C_i/C_a) and the transpiration rate (E)), chlorophyll *a* fluorescence parameters (maximum PSII quantum efficiency (F_v/F_m), photochemical yield (Y(II)), yield for dissipation by down-regulation (Y(NPQ)) and (Y(NO)) as well as electron transport rate (ETR), concentrations of chlorophyll *a* + *b* (Chl_{a+b}), carotenoids (CAR), activities of superoxide dismutase (SOD), catalase (CAT), peroxidase (POX), ascorbate peroxidase (APX), β-1,3-glucanases (GLU), phenylalanine ammonia-lyase (PAL) and polyphenoloxidase (PPO) and the concentrations of superoxide (O_2^-), hydrogen peroxide (H_2O_2) and malondialdehyde (MDA).

Figure 1. White mold symptoms (A-I), severity (J) and lesion area (K) determined for soybeans plants inoculated with *Sclerotinia sclerotiorum* (A-C), plants inoculated with *S. sclerotiorum* and sprayed with manganese phosphite (D-F) and plant inoculated with *S. sclerotiorum* and sprayed with Fluazinam (G-I). Means from each treatments, at each evaluation time, followed by different letters are significantly different ($P \leq 0.05$) according to the Tukey's test. Bars represent the standard error of the means. $n = 4$.

Figure 2. *In vitro* test of *Scletorotinia sclerotiorum* cultures in Petri dishes, illustrating the inhibition of mycelial radial growth with 0 (A) 1.25 (B), 2.5 (C), 5 (D) and 10 (E) ml L^{-1} of Mn phosphite concentration and 1.25 ml L^{-1}(F) of fluazinam concentration.

Figure 3. Leaf gas exchange parameters net carbon assimilation rate (*A*) (A and B), stomatal conductance to water vapor (g_s) (C and D), internal to ambient CO_2 concentration ratio (C_i/C_a) (E and F) and transpiration rate (*E*) (G and H) determined on leaflets of soybeans plants that were non-inoculated (A, C, E and G) or inoculated (B, D, F and H) with *Sclerotinia sclerotiorum* and non-sprayed (control) or sprayed either with manganese phosphite or Fluazinam. For each evaluation time, means from each treatment followed by different letters and for non-inoculated and inoculated plants for each treatment followed by an asterisk (*) are significantly different ($P \leq 0.05$) according to Tukey's test. Bars represent the standard error of the means. $n = 4$.

Figure 4. Images of chlorophyll *a* fluorescence parameters maximum PSII quantum efficiency (F_v/F_m), photochemical yield (Y(II)), yield for dissipation by down-regulation (Y(NPQ)) and (Y(NO)) determined on leaflets of soybeans plants that were non-inoculated or inoculated with *Sclerotinia sclerotiorum* and non-sprayed (control) or sprayed either with manganese phosphite or Fluazinam.

Figure 5. Maximum PSII quantum efficiency (F_v/F_m) (A and B), photochemical yield (Y(II)) (C and D), yield for dissipation by down-regulation (Y(NPQ)) (E and F), (Y(NO)) (G and H) and electron transport rate (ETR) (I and J) determined on leaflets of soybeans plants that were non-inoculated (A, C, E, G and I) or inoculated (B, D, F, H and J) with *Sclerotinia sclerotiorum* and non-sprayed (control) or sprayed either with manganese phosphite or Fluazinam. For each evaluation time, means from each treatment followed by different letters and for non-inoculated and inoculated plants for each treatment followed by an asterisk (*) are significantly different ($P \leq 0.05$) according to Tukey's test. Bars represent the standard error of the means. $n = 4$.

Figure 6. Concentrations of the photosynthetic pigments chlorophyll *a+b* (Chl_{a+b}) (A and B) and carotenoids (CAR) (C and D) determined on leaflets of soybeans plants that were non-inoculated (A and C) or inoculated (B and D) with *Sclerotinia sclerotiorum* and non-sprayed (control) or sprayed either with manganese phosphite or Fluazinam. For each evaluation time, means from each treatment followed by different letters and for non-inoculated and inoculated plants for each treatment followed by an asterisk (*) are significantly different ($P \leq 0.05$) according to Tukey's test. Bars represent the standard error of the means. $n = 4$

Figure 7. Activities of superoxide dismutase (SOD) (A and B), catalase (CAT) (C and D), peroxidase (POX) (E and F), ascorbate peroxidase (APX) (G and H), β-1,3-glucanases (GLU) (I and J), phenylalanine ammonia-lyase (PAL) (K and L) and polyphenoloxidases (PPO) (M and N) determined on leaflets of soybeans plants that were non-inoculated (A, C, E, G, I, K and M) or inoculated (B, D, F, H, J, L and N) with *Sclerotinia sclerotiorum* and non-sprayed (control) or sprayed either with manganese phosphite or Fluazinam. For each evaluation time, means from each treatment followed by different letters and for non-inoculated and inoculated plants for each treatment followed by an asterisk (*) are significantly different ($P \leq 0.05$) according to Tukey's test. Bars represent the standard error of the means. $n = 4$.

Figure 8. Histochemical detection of hydrogen peroxide (H_2O_2) at 96 hours after inoculation (A-F) and concentrations of superoxide (O_2^-) (G and H), H_2O_2 (I and J) and malondialdehyde (MDA) (K and L) determined on leaflets of soybeans

plants that were non-inoculated (A, B, C, G, I and K) or inoculated (D, E, F, H, J and L) with *Sclerotinia sclerotiorum* and non-sprayed (control) or sprayed either with manganese phosphite or Fluazinam. For each evaluation time, means from each treatment followed by different letters and for non-inoculated and inoculated plants for each treatment followed by an asterisk (*) are significantly different ($P \leq 0.05$) according to Tukey's test. Bars represent the standard error of the means. $n = 4$.

Table 1

Variables	P	PI	ST	P × PI	P × ST	PI × ST	P × PI × ST
WMS	<0.001	-	<0.001	-	<0.001	-	-
LA	<0.001	-	<0.001	-	<0.001	-	-
A	<0.001	<0.001	<0.001	<0.001	<0.001	<0.001	<0.001
g_s	<0.001	<0.001	<0.001	<0.001	<0.001	<0.001	<0.001
C_i/C_a	<0.001	<0.001	<0.001	<0.001	<0.001	<0.001	<0.001
E	<0.001	<0.001	<0.001	<0.001	<0.001	<0.001	<0.001
F_v/F_m	<0.001	<0.001	<0.001	<0.001	<0.001	<0.001	<0.001
Y(II)	<0.001	<0.001	<0.001	<0.001	<0.001	<0.001	<0.001
Y(NPQ)	<0.001	<0.001	<0.001	<0.001	<0.001	<0.001	<0.001
Y(NO)	<0.001	<0.001	<0.001	<0.001	<0.001	<0.001	<0.001
ETR	<0.001	<0.001	<0.001	<0.001	<0.001	<0.001	<0.001
CHL $a+b$	<0.001	<0.001	<0.001	0.007	<0.001	<0.001	<0.001
CAR	0.003	<0.001	<0.001	0.134	<0.001	<0.001	<0.001
SOD	<0.001	<0.001	<0.001	0.021	0.008	<0.001	<0.001
CAT	0.002	<0.001	<0.001	0.003	<0.001	<0.001	<0.001
POX	0.006	<0.001	<0.001	<0.001	<0.001	<0.001	<0.001
APX	0.210	<0.001	<0.001	0.336	0.148	0.001	0.143
GLU	<0.001	<0.001	<0.001	0.009	<0.001	<0.001	<0.001
PAL	<0.001	<0.001	<0.001	0.003	<0.001	0.002	<0.001
PPO	<0.001	<0.001	<0.001	<0.001	<0.001	<0.001	<0.001
O_2^-	0.020	0.431	0.102	0.101	0.207	0.006	0.003
H_2O_2	<0.001	0.318	0.010	<0.001	<0.001	<0.001	0.068
MDA	<0.001	<0.001	<0.001	<0.001	<0.001	<0.001	<0.001

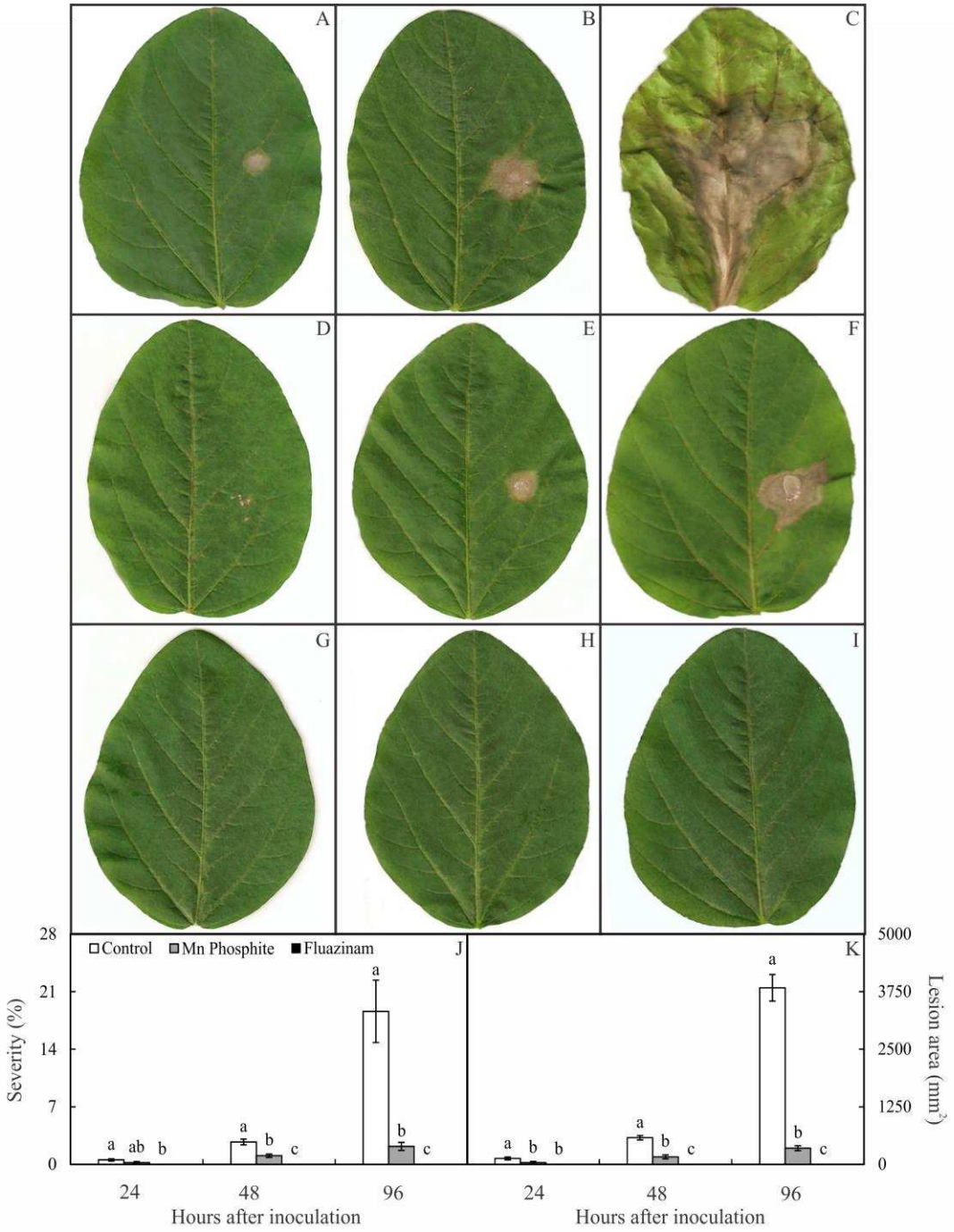
A
B
C
D
E
F
G
H
I
J
K
Control
Mn Phosphite
Fluazinam
Severity (%)
Lesion area (mm²)
28
21
14
7
0
5000
3750
2500
1250
0
a
ab
b
a
b
c
a
b
c
a
b
b
a
b
c
a
b
c
24
48
96
Hours after inoculation
24
48
96
Hours after inoculation

Figure 1

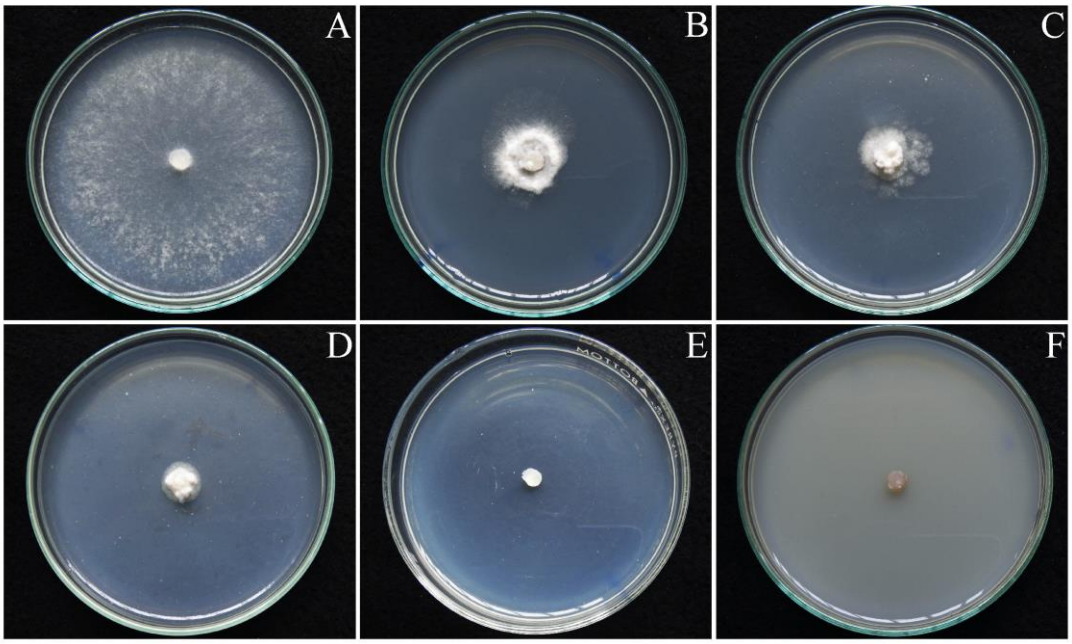

Figure 2

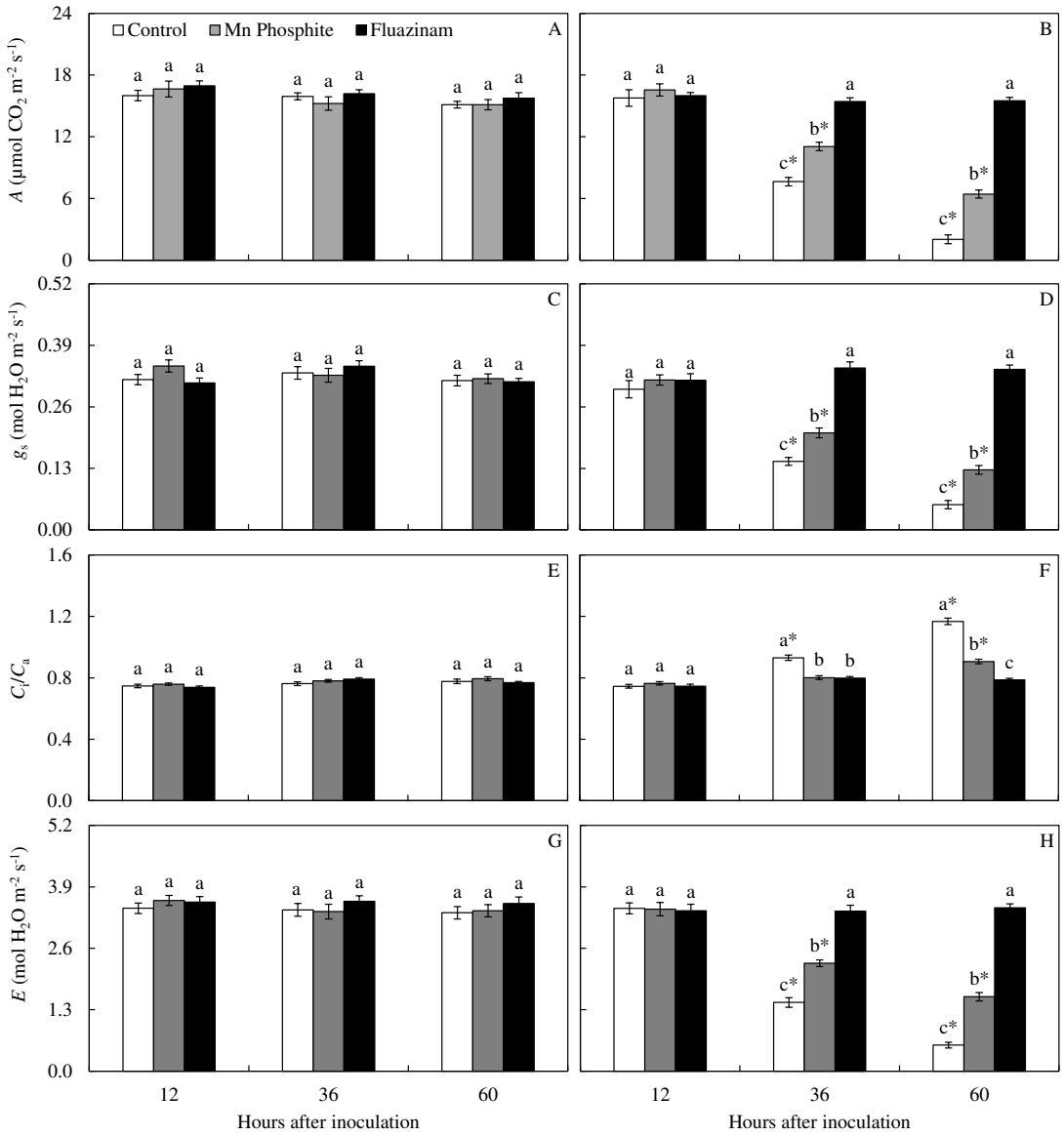
Control
Mn Phosphite
Fluazinam
A
B
C
D
E
F
G
H
A (μmol CO2 m-2 s-1)
gs (mol H2O m-2 s-1)
Ci/Ca
E (mol H2O m-2 s-1)
Hours after inoculation
Hours after inoculation

Figure 3

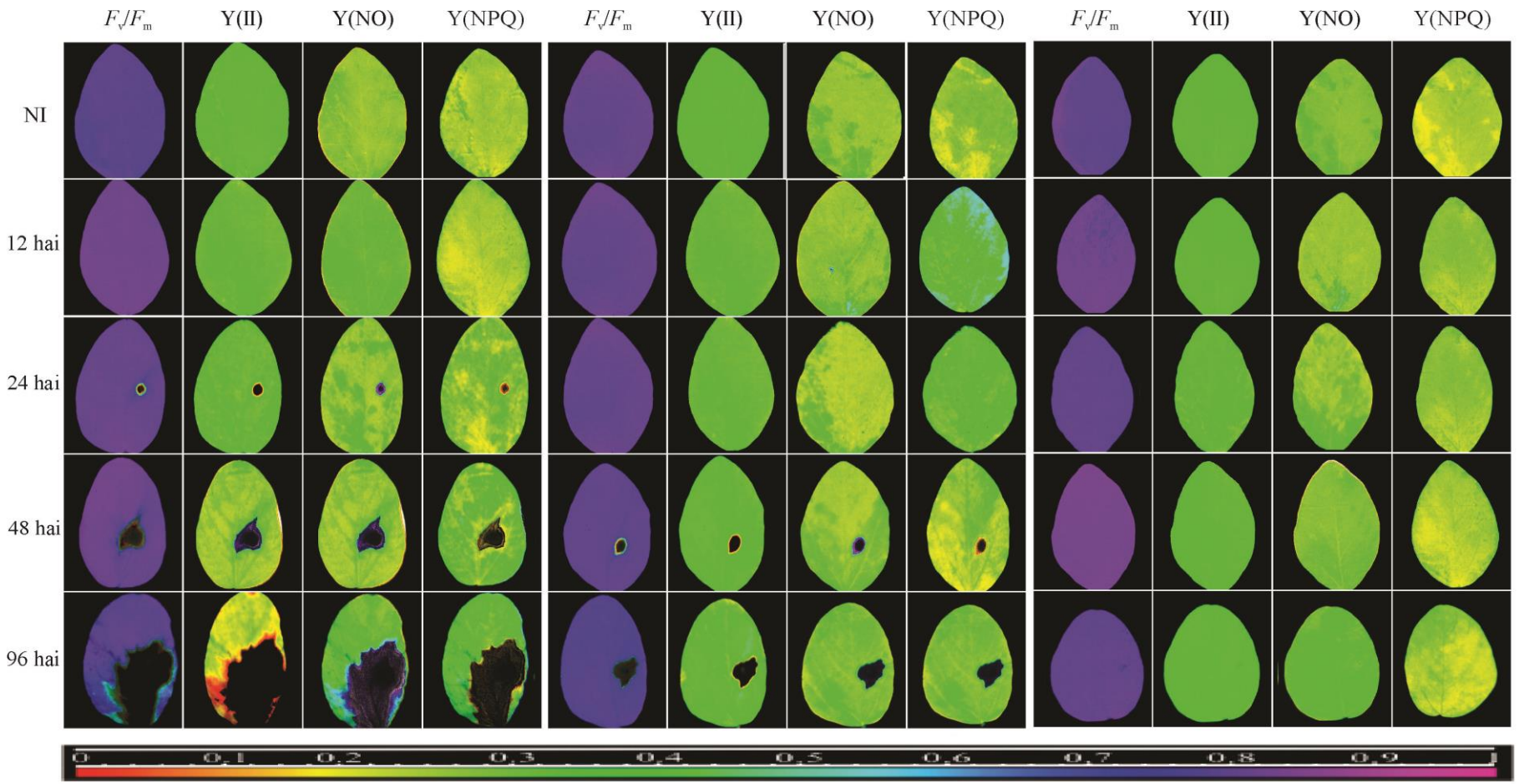
F_v/F_m
Y(II)
Y(NO)
Y(NPQ)
F_v/F_m
Y(II)
Y(NO)
Y(NPQ)
F_v/F_m
Y(II)
Y(NO)
Y(NPQ)
NI
12 hai
24 hai
48 hai
96 hai
0
0.1
0.2
0.3
0.4
0.5
0.6
0.7
0.8
0.9

Figure 4

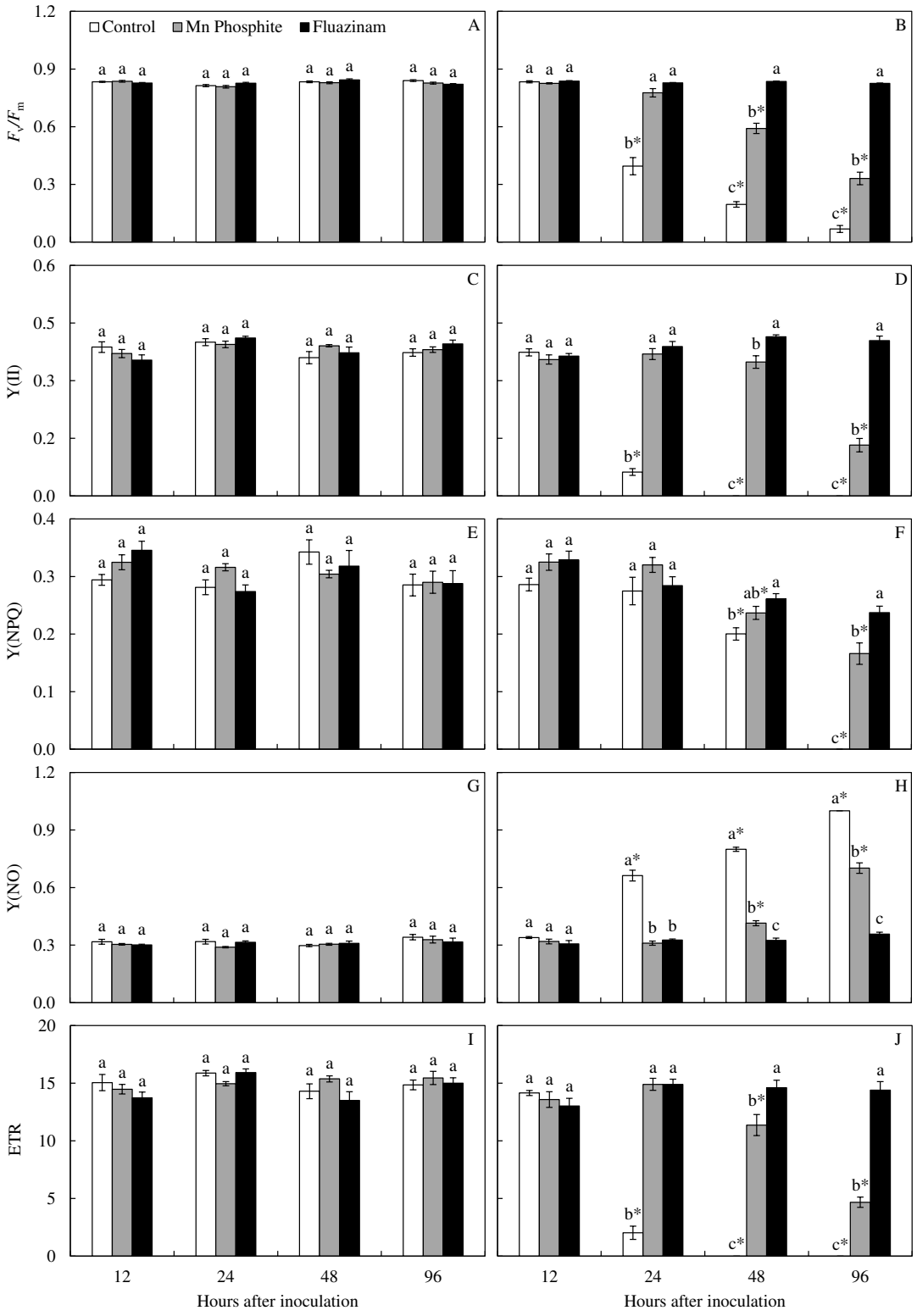
Control
Mn Phosphite
Fluazinam
A
B
C
D
E
F
G
H
I
J
F_v/F_m
Y(II)
Y(NPQ)
Y(NO)
ETR
12
24
48
96
Hours after inoculation
Hours after inoculation

Figure 5

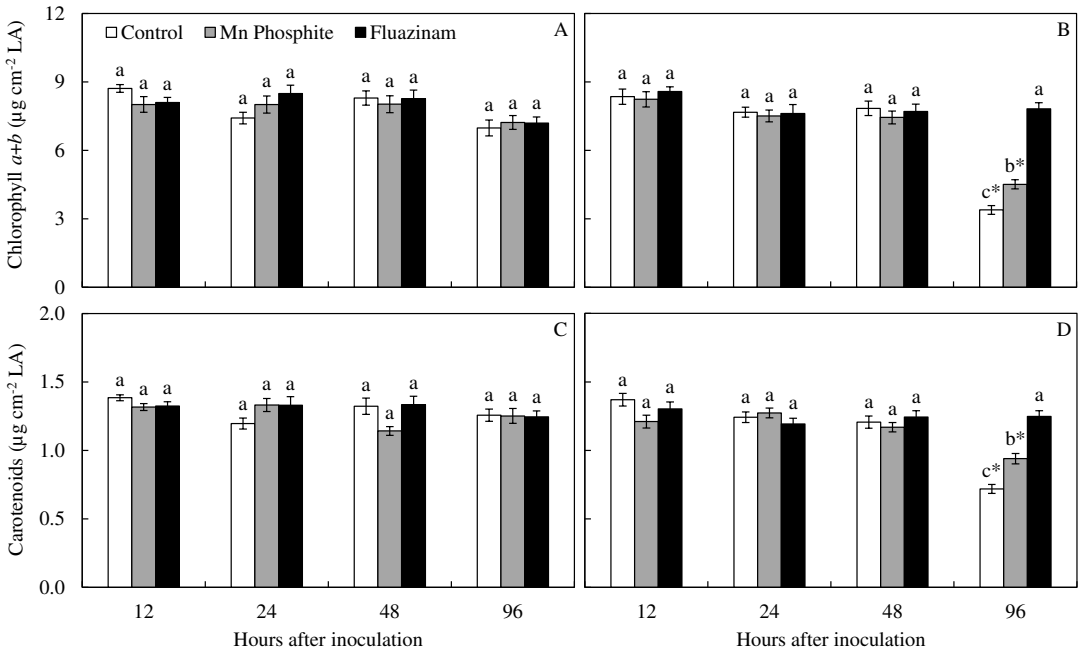
Control
Mn Phosphite
Fluazinam
A
B
C
D
Chlorophyll a+b (µg cm-2 LA)
Carotenoids (µg cm-2 LA)
Hours after inoculation
Hours after inoculation
12
24
48
96

Figure 6

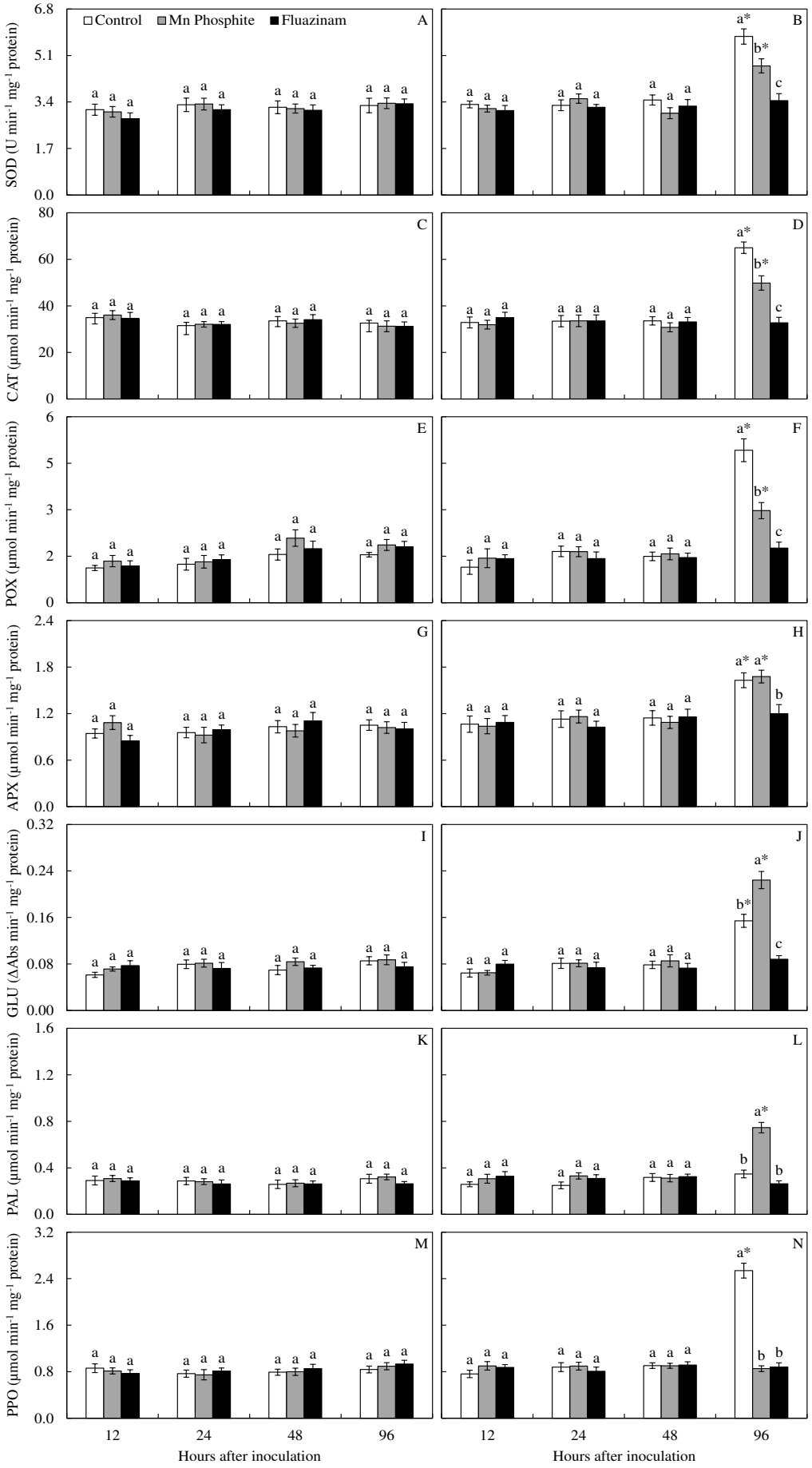
Control
Mn Phosphite
Fluazinam
A
B
C
D
E
F
G
H
I
J
K
L
M
N
SOD (U min-1 mg-1 protein)
CAT (μmol min-1 mg-1 protein)
POX (μmol min-1 mg-1 protein)
APX (μmol min-1 mg-1 protein)
GLU (ΔAbs min-1 mg-1 protein)
PAL (μmol min-1 mg-1 protein)
PPO (μmol min-1 mg-1 protein)
12
24
48
96
Hours after inoculation
Hours after inoculation

Figure 7

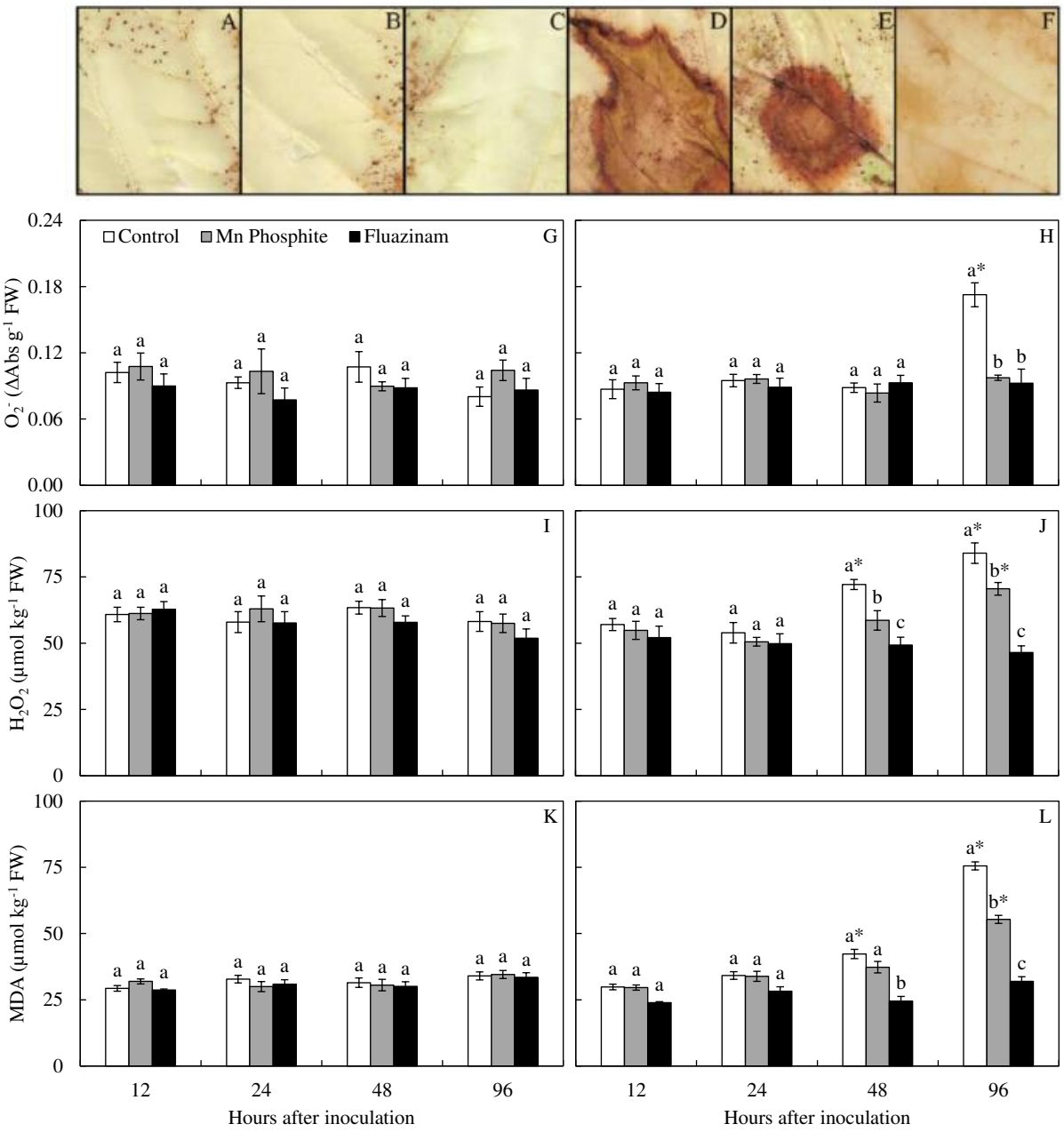
A
B
C
D
E
F
Control
Mn Phosphite
Fluazinam
G
H
I
J
K
L
O_2^- (ΔAbs g^{-1} FW)
H_2O_2 (μmol kg^{-1} FW)
MDA (μmol kg^{-1} FW)
0.24
0.18
0.12
0.06
0.00
100
75
50
25
0
12
24
48
96
Hours after inoculation

Figure 8